Phylogeography of the cryptic species complex: Araneus bogotensis

Juan Sebastián Sarmiento Cepeda

Universidad del Rosario
Facultad de Ciencias Naturales
Bogotá, Colombia
2024

Phylogeography of the cryptic species complex: Araneus bogotensis

Juan Sebastián Sarmiento Cepeda

Daniel Garrido

Jimmy Cabra

Fabian Salgado

Camilo Salazar

Artículo presentado como requisito para obtener el título de:

Biólogo

Director

Camilo Salazar

Facultad de Ciencias Naturales
Biología
Universidad del Rosario
Bogotá, Colombia
2024

Abstract

Background

Explore the biodiversity of any taxon is an important task to disentangle the three of life. Genetics is a powerful tool to uncover biodiversity that eludes visual observation. Identification of cryptic species complexes has experienced a recent increase in the literature due to the inclusion of different types of genetic markers. However, there is still an important research gap in arachnids, where several morphospecies still lack genetic data and few studies explore the effects of biogeographic barriers in shaping their diversity. Spiders are well known to be important ecosystem regulators, yet some genera remain poorly studied. *Araneus bogotensis*, commonly known as a garden spider, exhibits a broad distribution in the Andes. Current classifications have approached it with caution due to its considerable morphological variation, making it an intriguing subject for investigation. We hypothesized that this species has a complex evolutionary history with multiple cryptic lineages.

Methods

To test this hypothesis, we sequenced mitochondrial and nuclear markers, estimated divergence times, ran demographic and species delimitation models and employed a morphometric analysis.

Results

Our findings revealed three independent structured lineages that cannot be differentiated by current taxonomic keys. The first lineage comprised most of Colombian populations here sampled, named here as *Araneus bogotensis sensu*

stricto, the second lineage, with an estimated divergence time of 10.9 Mya, comprised individuals from a single population in Serranía del Perijá, North Colombia and the third and oldest lineage comprised a Southern Brazilian population with 18.5 Mya time of divergence. Furthermore, the analyses showed an additional four divergent lineages within *A. bogotensis sensu stricto* structured by the Magdalena River Valley acting as a strict barrier to gene flow.

Conclusions

Our findings revealed cryptic species within what is called Araneus bogotensis, where the geomorphology of the Andes plays an important factor to lineages demography and diversification in Colombia and South America.

Introduction

Addressing the real diversity of a taxa it's important to understand the history, evolution and ecology of the species (1,2). Formerly, we used to rely on morphology to delimitate species, but genetic data has recently increased our ability to uncover hidden diversity, especially when facing Cryptic Species Complexes (CSC) (3). Defined by Bickford (4), a CSC is when two or more species were once "classified as a single nominal species because they are at least superficially morphologically indistinguishable". This phenotypic convergence can be explained through different evolutionary processes: i. divergent evolution, where different loci cause the same phenotype in independent lineages, ii. parallel evolution, where different alleles at the same locus cause the same phenotype, this also includes when a mutation has appeared multiple times, and iii. collateral evolution, where species share alleles with one another either due to ancestral polymorphism or by introgression (5). Although there are studies showing that CSCs are widely distributed across taxa (6), there are still few studies in spiders exploring this issue. Even less if we compare neotropical with temperate regions (4).

An important factor to assess species' diversification is the landscape changes across time (7). Andes has configured the geomorphology of South America since its initial rise ~65 Mya, introducing foreland basins and critical elevation mountains (8). For that reason, Andes has been linked to speciation processes mainly due to vicariance but also to dispersal events (9–13). Divergence times coinciding with geographical barriers' formation may suggest vicariance events (14), meanwhile divergence times surpassing the barriers' formation may indicate dispersal events

(15). For lowland species, mountains can act as biogeographical barriers. On the other hand, for highland species, basins and rivers could represent biogeographical barriers (15). For example, rivers within the Amazon basin have been identified as a geographical barrier, limiting gene flow and promoting speciation for many taxa (16–18). Smaller basins, such as the Magdalena Basin have also been linked with species diversification events before (19). Nevertheless, there are many cases in which these barriers have proven permeable, allowing dispersal events across the barrier (20–22), in which flight or ballooning (a behavior documented in spiders) could explained crossing water bodies' barriers (21,23).

The identification of cryptic species is regularly difficult since they tend to be distinguishable only by non-visual traits, such as mating signals and calls (4,24) and that is why this variation might elude visually oriented taxonomists (4). In the realm of arachnids, where visual interspecific communication is of lesser importance in most taxa, speciation processes can take place with minimal morphological change (25,26). Thus, molecular analyses in arachnids consistently reveal new divergent cryptic lineages (27–34). For example, five species of tarantulas, previously named as *Antrodiaetus rivesi* were accurately identified by amplicon sequencing as different species in Central California (34). A tarantula from the same genus named *A. unicolor*, was reported to have a CSC with a non-sister species (30).

The Araneidae family has more than 3100 species across 170 genera (World Spider Catalog, 2023 (35)), ranking the third largest family within the order Araneae. Surprisingly, only a handful of genera within this extensive family has been previously studied in the American Neotropics, including *Trichonephila* (36,37),

Gasteracantha (38–40) and *Micrathena* (41–43). The genus *Araneus*, basionym of the family and the order Araneae, is the largest spider genus with 641 species (44). Despite its amazing size, the genus remains relatively unexplored. A major study conducted by Scharff et al. (44) aiming to clarify the phylogenetic relationships within Araneidae, found evidence for the establishment of seven new genera with only 11 *Araneus* spp. This spotlight how polyphyletic this genus really is and how under studied it remains.

To date, several studies have looked into non-tropical *Araneus* spp. (44–50), but only two studies have employed genetic data to evaluate phylogeographical hypotheses in Neotropical *Araneus* species. Peres et al. (51) showed that *Araneus omnicolor*'s demography was not significantly influenced by climatic changes during the Last Glacial Maximum and Minimum. Instead, other factors may have contributed most to their current population dynamics such as the species' dispersal ability. In a second study, Peres et al. (52) demonstrated that rearrangements of Neotropical forests during the Tertiary and Quaternary periods had a substantial influence on the populations dispersal and subsequent divergence of the species *Araneus venatrix* in Brazil.

Araneus bogotensis, an orb-weaver spider first described in 1864 by Keyserling, inhabits Andean and sub-Andean regions, with a reported altitude interval between the 140 and 4000 meters above sea level, which makes it a premontane to montane species. Two observations suggest that this species may be a CSC. First, it exhibits a broad distribution across the Andean mountain system, from Northern Colombia to Bolivia, with isolated records along the East South Coast of Brazil (53). Second,

it presents a wide morphological variation, not only in overall morphology but also in diagnostic traits. Levi (53) described populations that lacked the two-line characteristic abdomen pattern and noticed that this species displayed an unusual wide range of body sizes, with females ranging from 6.8 mm to 12.8 mm and males from 4.5 mm to 7.9 mm.

The aim of this study is to determine whether *A. bogotensis* populations have structure lineages fitting into a CSC description, employing both genetic and morphological evidence. Genetic data included three genes -COI, ITS2 and 28S-, used to estimated phylogenetic trees, haplotype networks, diversity and structure summary statistics, genetic distances, and to implement demographic and gene flow models. Morphological data was based on the shape and size of the female epigynum, a common diagnostic trait for species identification, to conduct a morphometric analysis. We hypothesized that *A. bogotensis* phenotypic variation is not correlated with genetic variation. Therefore, we expected to observe several genetically structured lineages, that present a common morphology, aligning with a CSC description. Furthermore, given the Andes complexity in Colombia we anticipated that the diversification of these lineages were influenced by the geomorphology of the region. This investigation represents a valuable contribution to spiders' evolution and taxonomy in South America as it reveals several new lineages and allows to study in depth drivers of diversification in the region.

Methodology

Sampling

Our geographic sampling spanned a part of the known distribution of *A. bogotensis* (n = 237 individuals) from 19 different localities in Colombia (see Figure 1) and from several species of the genus, from which the sequences were available on Genebank (Appendix 1). We used a dichotomous key from Levi, 1991 (53) for the determination of the individuals. Populations of *Araneus* species in Colombia were sampled by searching on curled leaves, a typical behavior in this species. The specimens were then fixed in 90% ethanol and stored in – 20 °C freezers. One picture of the abdomen's morphotype was taken from each locality (see Figure 1). We sequenced 56 individuals (see Appendix 1) and dissected and photograph 107 female's epigynum for morphometric analysis. There were 84 juveniles who could not be identified due to no existing juvenile taxonomic keys and 16 mature males that were mostly from one population. All specimens were deposited at the Museo de Entomología de la Universidad del Valle (RNC: 077).

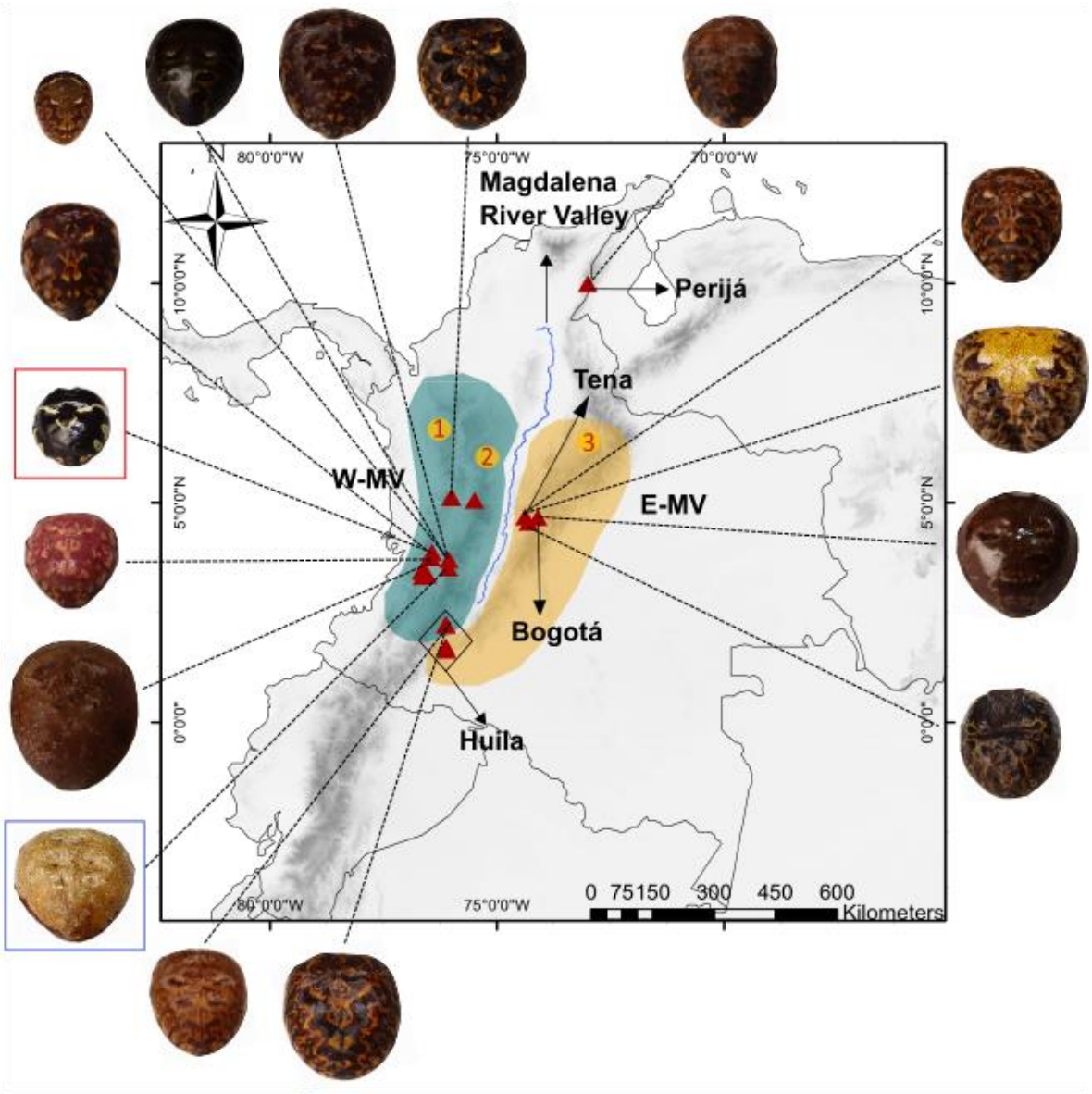

Figure 1: Sampling map with abdomen morphotype from each locality. Yellow circles with numbers 1, 2 and 3 indicate West, Central and East cordilleras from Colombian Northern Andes respectively. Abdomens inside red and blue squares, represent the 34_BosquedeNieblaSanAntonio_Cali and Palmira individual's morphotype, respectively.

DNA extraction, amplification and sequencing

We used three DNA fragments: the mitochondrial cytochrome oxidase 1 (COI; 506 bp), the nuclear Internal Transcribed Spacer subunit 2 (ITS2; 528 bp) and the ribosomal gene 28S (28S; 847 bp). For COI, we used LCO1490 and HCO2198 primers (54), for ITS2, we used 5.8 and 28S primers (55) and for 28S, we used 28SO and 28SC primers (56) (see Supplementary Table 2). The PCR conditions for COI and ITS2 fragments are described in Salgado-Roa *et al.* (39). For the 28S PCR the conditions were the following: 95°C for 10 minutes, 35 cycles at 95°C for 45 s, 56.6°C for 45 s and 72°C for 60 s; and a final extension at 72°C for 10 minutes. Positive amplicons were visualized on a 1% agarose gel, purified with Exo-SAP and bidirectional sequenced by Macrogen Inc. Base calls and assemblies were performed in Geneious Prime 2022.2.1 (www.geneious.com). For individuals with heterozygous calls in COI and 28S sequences, we carry out an haplotype inference with PHASE (57) implemented in DnaSP v.6.12.03 (58), with 5000 iterations per simulations, accepting those haplotypes with > 90% confidence.

Given the known intronic variability of the ITS2 fragment we decided to use a high-fidelity polymerase LongAmp Taq 2X Master Mix (New England BioLabs) and MinION (Oxford-Nanopore) sequencing for this molecular marker. We prepare the library using Native Barcoding Kit 96 V14 (SQK-NBD114.96), then it was cleansed with AMPure XP beads (Beckman Coulter). The quality of the total reads was assessed with Nanostat (59) and then filtered with a Q = 14 cut-off. Clusters of the reads having 95% identity were obtain with isONclust (60) to obtain the two alleles

per individual. The sanger and MinION obtained sequences were aligned to obtain the marker dataset.

The alignments were carry out in AliView v.1.28 (61) using MUSCLE algorithm, then they were visually inspected and corrected in the same software. For the two coding loci, we checked for possible stop codons on MEGA (62).

Phylogenetic reconstruction and divergence times estimation

For the phylogenetic analysis, in the ML matrix we included all the sequences from the genus *Araneus* found in Genbank (june 2023), and in the BI matrix we left out the ones classified as *Araneus* Holartics 2 in the ML tree (see Appendix 1). Phylogenetic relationships between populations of *A. bogotensis* and the complete dataset were estimated through a Maximum Likelihood (ML) in IQ-Tree v.1.6.12 (63) and Bayesian Inference (BI) in BEAST v.1.8 (64). The outgroups used were species from the same family (Araneidae) *Zygiella keyserlingi, Witica cayanus, Rubrepeira rubronigra, Alpaida carmínea* and *Cyclosa conica* (see Appendix 1). The topology of ML tree was estimated for each locus and for a multiple concatenated alignment, both in IQ-Tree v.1.6.12 (63). To create the concatenated alignment we used FASconCAT-G v.1.05 (65) joining every nuclear allele sequence of every individual to the same mitochondrial individual's haplotype. We used ModelFinder from IQ-Tree to select the best fitted substitution model based on the Bayesian Criterion Information (BIC) for each locus. Node supports were calculated using 10.000 UltraFast Bootstrap pseudoreplicates.

We obtain a Maximum Credibility Clades tree and estimated divergence times with BEAST v.1.8 (64) using only the mitochondrial alignment, since many of the

individuals from other species did not have the ITS2 and 28S sequences available. We selected the best fitted molecular clock model based on the likelihood comparison test implemented in MEGA11 (62). We use a Birth-Death model with a relaxed Log-normal molecular clock (66). We specified two priors, the mean age of the MRCA of Araneidae family, of 70 Mya, Sd: 28 My (37,38) and the substitution/site/million years rate which has a mean of 0.0112 and Sd: 0.001 (37,67,68). We ran 100 million generations, sampling every 1000 generations. We used TRACER (69) to confirm the convergence of the chains to a stationary distribution, verifying that every effective sample sizes of the parameters were superior to 200. Finally, we used TREANNOTATOR (64) to compute a maximum credibility tree having 20% of the trees as burn-in.

Species delimitation

We implemented a species delimitation test that Integrates genes and traits in a Bayesian Phylogenetic and Phylogeography (iBPP) coalescent method (70) which allows to join the morphometric and the molecular dataset. As there were no epigynum morphometric measures available for other *Araneus* species, we include only our populations morphometric data (see Morphometric geometry section). This data consisted of 12 PCs that resume ~90% of the total variation of the epigynum. We ran iBPP under nine parameter combinations of prior distributions for the ancestral population size and the root age (τ) ranging from scenarios that represent large population sizes and a deep divergence times (θ = G(1,10) and τ = G(1,10)) to those representing small population sizes and a shallow divergence time (θ = G(2,2000) and τ = G(2,2000)) as previously implemented in other arthropods (71–

73). The MCMC analysis was run over 50.000 iterations, sampling every 1000 steps, and using a 10% burn-in. The parameters of the locus-specific rates of evolution were fine-tuned using an auto-option.

Populations Genetics

For every loci we calculate different summary statistics in DnaSP v.6.12 (58) in order to characterize the genetic variation of *A. bogotensis'* populations such us: nucleotide diversity (π), haplotypic diversity (H_d), segregant sites (S), the population substitution rate (θ), Tajima's D and Fu and Li's D for geographic zones and clades (see Table 1 and Supplementary Table 3). The genetic differentiation was estimated between Perijá, E-MV and W-MV using a relative measure (F_{ST}) and two absolute measures (D_{xy} and D_a). Population structure (F_{st}) vs. the null hypothesis of panmixia was evaluated with the Hudson permutation test (74) with 5000 replicates. Haplotypes relationships between *A. bogotensis* lineages and by geographic zones, was obtained by statistically parsimony networks (TCS) using PopArt v.1.7 (75).

The level of clustering from the genetic variation of each sample was determined with Structure 2.3.4 (76). We ran 150.000 Markov chain Monte Carlo (MCMC) generations, with 50.000 MCMC as burn-in. We tested 1 to 19 number of clusters (K), with 20 iterations for each K value. The selection criteria of the best fitted K followed two complementary methods (77): i. according to Evanno method (78), ii. Visualizing the log likelihood vs K-values (79). Barplots with K=2 and K=3 were generated with POPHELPER R package (80).

We explore spatial patterns of genetic variation using several approaches. Firstly, we assessed isolation by distance implementing a Mantel test in R package vegan

(81). We used linearized distances among localities with a Fst transformation (1/1-Fst) and the geographical distances were calculates using distm from the geosphere package (82). Secondly, patterns of migration of *A. bogotensis* in Colombia were inferred with the effective geographic migration surfaces obtained from the EEMS software (83). The potential distribution of the species in Colombia based on the altitudinal threshold previously reported for *A. bogotensis* (53) served as the study area polygon. This polygon was constructed using Google Maps API v3 Tool (http://www.birdtheme.org/useful/v3tool.html). We used 200 hundred demes. The software ran 2 million MCMC, sampling every 10.000 steps and discarding the first 50% as burn-in. The results were then visualized using rEEMSplot2 package from R as suggested by Petkova (83). Thirdly, we checked if the low gene flow surfaces obtained with EEMS correspond to possible geographic barriers implementing the Monmonier´s algorithm (84) in the R package *adegenet* (85), adopting the Delaunay triangulation.

Demographic models

Based on the phylogenetic and population genetics results, we implemented a model-based approach to evaluate divergence within the two geographic groups from *A. bogotensis s.s.*. We ran PHRAPL (86) and selected the demographic model that best fit the topologies of the individual trees from each locus. This software calculates a proportion of the time a model fit the topologies obtained which can be seen as a log-likelihood, then it computes an Akaike Information Criterion (AIC) as a lack of fit to a specific model and finally a weighted AIC (wAIC) which represents the probability of adjustment, giving us a parameter to choose the suited model. We tried

6 different models, one that assumes isolation between geographic zones (west from Magdalena Valley and east from Magdalena Valley) with a single coalescent event and no migration, the second and third assume unidirectional migration, the fourth assumes bidirectional migration, the fifth and sixth assumes bidirectional asymmetrical migration (see Figure 10).

We used a tree for each locus, employed 4 tips and 100 locus subsamplings, giving as a result 300 trees. We ran a 100.000 trees simulation having the following parameters for every model: divergence times (t = t = 0.3, 0.58, 1.11, 2.12, 4.07), and migration times (m = 0.1, 0.22, 0.46, 1, 2.15) in 4 N y 4 Nm units, respectively.

Morphometric geometry

Given the small number of male samples collected we include only adult females for this analysis. We dissected the epigynum of 107 females, cleared them with clove oil, mounted on a microscope well slide and photographed their ventral view. We used a Nikon microscope coupled with a Leica camera and took the shots with a Leica software. For all photographs we used the same magnification, 10X ocular, 4X objective. Helicon Focus 8 (Kharkiv, Ukraine) was used to produce extended focal range images for each sample.

Landmarks generation was performed with tpsUtil v 1.81 y TpsDig v 2.32 (87). We used type I and type II landmarks to represent points of maximum and minimum curvature of anatomical features and points of intersection between anatomical features. We used semilandmarks to represent the outline of the spermathecas and the lateral plates. To prevent information loses we placed landmarks in both sides of

the spermathecas and lateral plates despite the fact these are symmetrical structures (88).

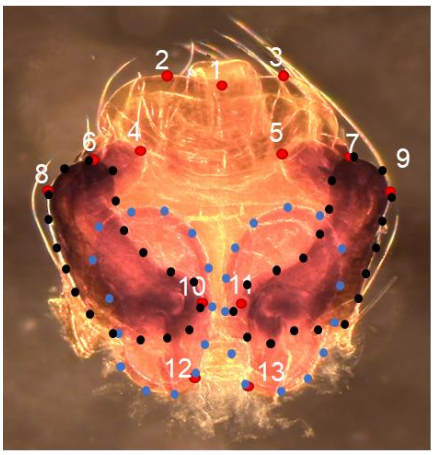

Number	Type	Description
1	II	Postero-median central point of the median plate.
2 (left), 3 (right)	II	Point of minimum curvature of the median plate posterior border.
4 (left), 5 (right)	II	Point of maximum curvature of copulatory ducts after the opening.
6 (left), 7 (right)	II	Point of maximum curvature in the lateral plate posterior border.
8 (left), 9 (right)	II	Point of maximum curvature in the lateral plate ectal border.
10 (left), 11 (right)	I	Intersection between the anterior region of the copulatory ducts and the spermatheca.
12 (left), 13 (right)	I	Intersection between the spermatheca anterior border and the fertilization duct.

Figure 2: Type and description of the landmarks used to measure the epigynum. Type I are points of minimum and maximum curvature on an anatomical feature. Type II are intersections between anatomical features. Blue a black points represent semilandmarks to get the spermatheca and lateral plates information.

Epigynum shape variability across samples was captured with the following analysis. We performed a Generalized Procrustes Analysis (GPA) to remove variation due to rotation, translation, and isometric size, retaining only shape variation. The sliding method was used to treat semilandmarks which minimizes the Procrustes distances between them. After that we carried out a symmetric analysis specifying the paired landmarks in the structure (see Figure 2) and remove the variation from the asymmetrical component to help in correcting the differences that come from angle deviation in the photos. These data were used to carrier out a principal component analysis (PCA) with Geomorph R package (89). We plotted the first two components that explains 25.26% and 15.52% of the variance. We evaluated the presence of

groups with a discriminant principal components analysis (DAPC) with adegenet v 2.1.10 (85) introducing the geographic zones as a prior classification to test shape differences between them.

To check shape differences were not a result of allometric change, we implemented a Procrustes ANOVA with 1000 permutations, to assess the variation and covariation of shape with centroid size and geographic zones as factors. No significant variation in shape was found by the interaction between the centroid size and the geographic zones so we performed an allometric correction removing the variation of shape due to centroid size.

Finally, we implemented a model-based Hierarchical Clustering using the best two components from PCA to calculate the group assignment probability of individuals regardless of *a priori* assignments with the *Mclust* (90). Maximum likelihood (ML) estimates of the alternative mixture models that describe morphometric variation in the data were obtained by expectation maximization (EM) algorithm. The optimal number of clusters were selected by Bayesian information criterion (BIC) and all models were evaluated for a predefined number of 1 to 9 clusters.

Results

Molecular phylogenetics and divergence time

The most suitable substitution models for COI, ITS2 and 28S were GTR+F+I+G4, SYM+I+G4 and TIM2+F+R5 respectively. The ML and BI topologies were generally concordant, topological differences were in part due to absence of some species between the ML and the BI analysis (e.g. *A. vincibilis, A. ejusmodi* and some holartic

species) and the fact that BI topology was only obtained from mtDNA. Both revealed the presence of three main clades within what is called *Araneus bogotensis*. The first clade, hereinafter referred to as "*Araneus bogotensis sensu stricto*", comprises the majority of samples collected in Colombia. The second clade, sister to the first one, contains all the sequences from Serranía del Perijá in Guajira, Colombia and a Brazilian species, *Araneus Blumenau*. These two clades are estimated to have diverged approximately 10.9 Mya (95% HDP = 3.1-30.7 Mya; see Figure 4). The third clade, sister to the other two, was composed of two subclades: one of them composed with Holarctic species 1 (*A. diadematus*, *A. acusisetus*, *A. marmoreus*, *A. trifolium*, *A. variegatus*, *A. ishisawai*, *A. stella* and *A. uyemurai*) and the other included *A. bogotensis* from Brazil, closely related to *A. omnicolor* and these two species were sisters with *A. workmani*. In the BI this last clade changes with *A. workman*i sister to *A. bogotensis* from Brazil and these two sisters to a clade composed by *A. vincibilis* and *A. omnicolor* (see Figures 3, 4). It is important to note that *A. omnicolor*, *A. workmani* and *A. vincibilis* are Brazilian species. ML and BI topologies also recovered the Holarctic species as paraphyletic, because in the ML, *A. ejusmodi* is sister to a clade composed of Brazilian species (*A. tijuca* and *A. venatrix*), and in the second, *A. acusisetus* was sister to the Brazilian species (see Figure 4). Finally, last clade named Holarctic species 2 (*A. pentagramicus*, *A. amabilis* and *A. mitificus*) in the ML topology appeared monophyletic and sister to all the other clades (see Figure 3). In the BI topology we do not have representatives of this clade and perhaps for this reason the Brazilian clade composed by *A. tijuca* and *A. venatrix* was the most external clade in this analysis but with low posterior probability (see Figure 4).

Within *A. bogotensis s.s.*, four internal clades were identified. The first clade comprises individuals from the Colombian West and Central Cordilleras, thereafter defined as the West Magdalena Valley group (W-MV; see Figure 1), this group diverged approximately 4.93 Ma (95% CI= 1.2-18.1 Mya; see Figure 4) from Tena clade. The second clade, which is sister to the previous clade, includes mixed individuals from two populations located in the East Cordillera: Tena, Cundinamarca, and La Plata, Huila, a population situated near to the Colombian Massif (see Figure 1). The later population presents a divergent pattern itself, since two individuals fell into the W-MV clade and the other two fell into the Tena clade (underlined individuals in Figure 4). The third clade is composed of individuals from Bogotá, also located in the East Cordillera, and is sister to the four and last clade, which consists of only two individuals, both from Valle del Cauca: one collected in Cali (34_BosquedeNieblaSanAntonio_Cali) and the other from El Cerrito (3_TenerifeelPailon_ElCerrito), thereafter named as the Fourth clade. The second and third clades, comprising Tena and Bogotá samples, will be collectively referred to East Magdalena Valley (E-MV) group for certain analysis since they appeared to be structured from the rest populations as we will see later on.

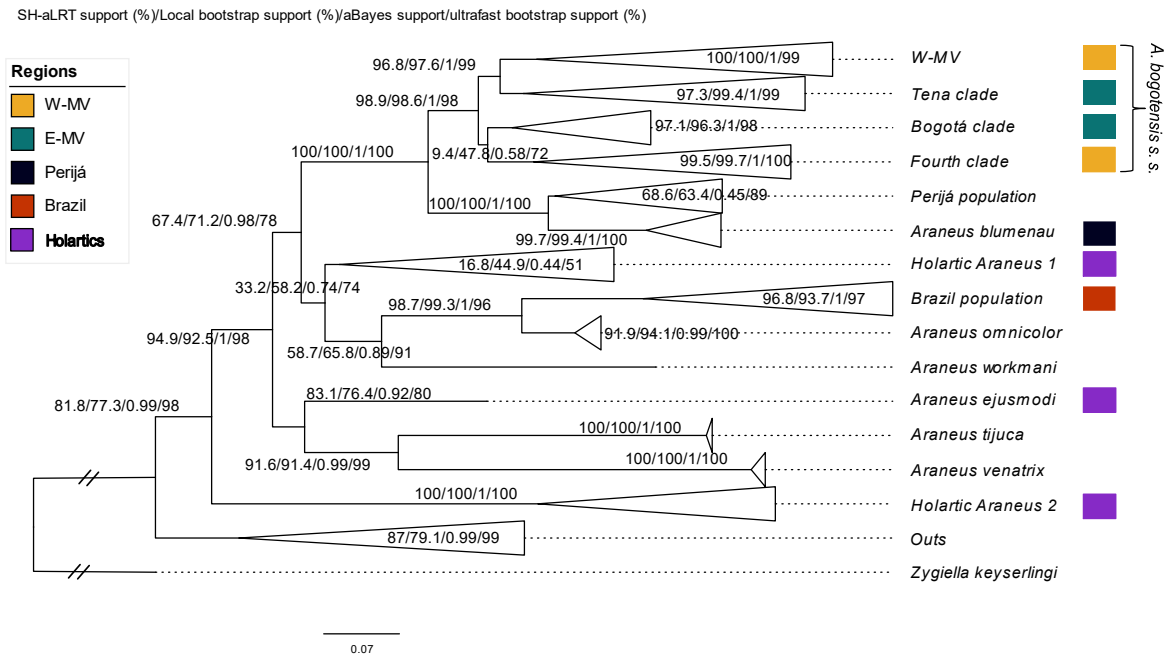

Figure 3: Concatenated phylogeny based on Maximum Likelihood algorithm. The node supports corresponds to SH-aLRT (%), local bootstrap (%), aBayes and untrafast bootstrap (%) respectively. The different regions West Magdalena Valley (W-MV), East Magdalena Valley (E-MV), Perijá, Brazil and Holarctic clades are colored next to the clades' names. A square bracket indicates the *A. bogotensis sensu stricto* group.

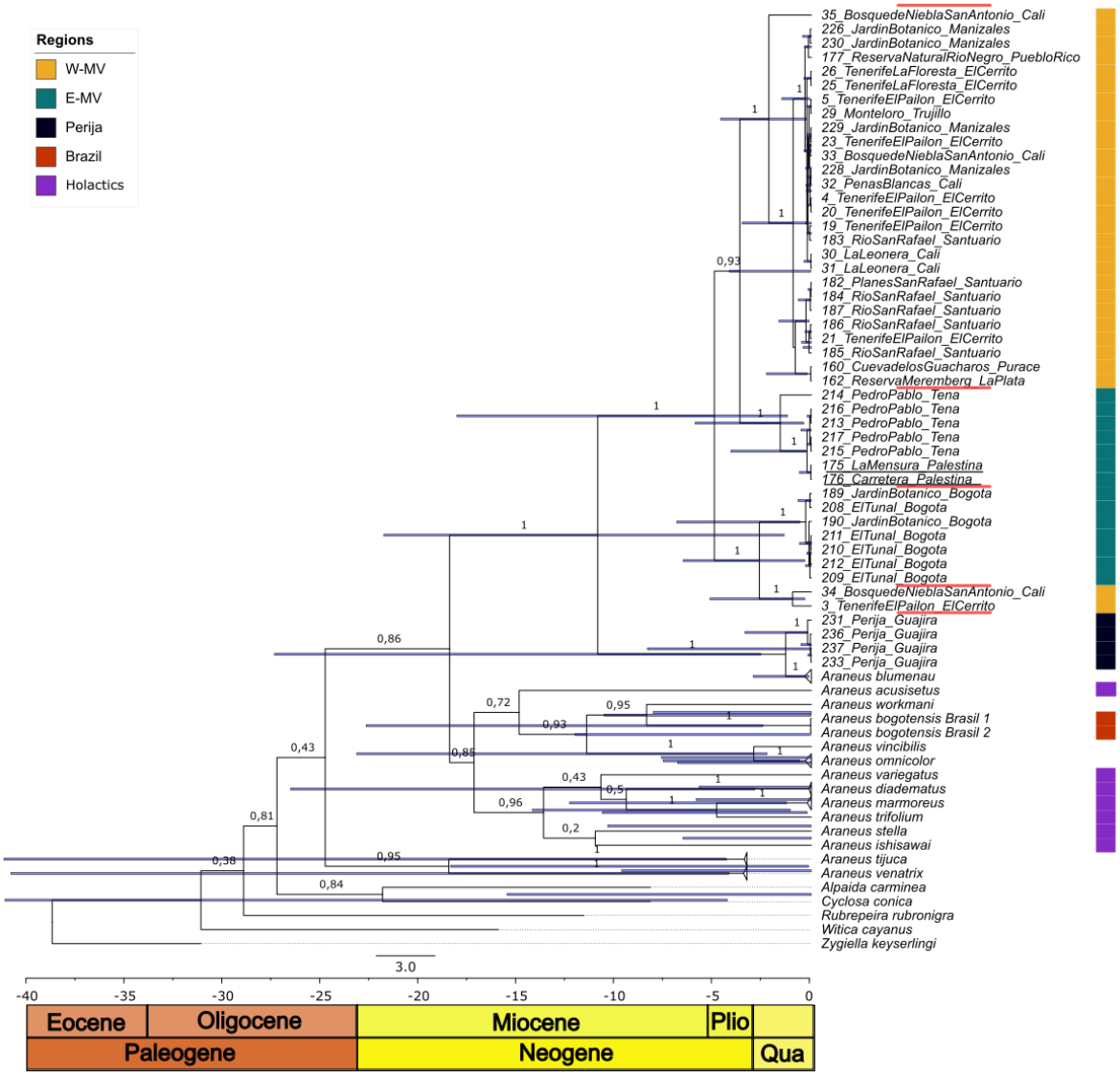

Figure 4: Mitochondrial phylogeny and Bayesian estimation times. Node support represents posterior probabilities. Horizontal blue bars illustrate the 95% HDP for the node's divergence times. The boxes in the bottom represent the geologic periods. Individuals are colored with the region where they come from. Numbers on top of geologic periods represent millions on years. Underlined names represent Huila individuals in Tena clade.

Genetic diversity and structure

Most neutrality tests conducted across the three loci did not yield statistically significant results, with an exception on ITS2 marker on W-MV group, suggesting neutral evolution across loci. Genetic diversity (π), within the COI and ITS2 regions, exhibits higher values in E-MV than in W-MV. However, in the case of 28S locus the genetic diversity was higher in W-MV (Table 1).

	COI (506 bp)			ITS2 (626 bp)		28S (847 bp)		
	West	East	Guajira	West	East	West	East	Guajira
N	29	14	4	61	28	42	24	8
Hd	0.897	0.857	0.5	0.962	0.997	1	1	1
pi	0.027	0.036	0.002	0.024	0.0559	0.058	0.036	0.059
theta	0.039	0.026	0.002	0.071	0.09	0.079	0.042	0.055
SS	73	42	2	78	88	211	102	88
Tajima's D	-1.227	1.658	-0.709	-2.299	-1.477	-1.005	-0.561	0.356
Fu and Li's I	0.2	0.718	-0.709	-3.532	-1.982	-0.698	-0.256	0.575

Table 1: Population genetic summary statistics from genetic groups for each locus. N: number of sequences, Hd: haplotype diversity, pi: nucleotide diversity per site, theta: expected nucleotide diversity per site, SS: segregating sites. Highlighted values are statistically significant with P-value < 0.05.

In the haplotype TCS networks, *A. bogotensis s.s.*, Perijá population and Brazil population were recovered with divergent haplotypes. For example, in COI, Brazil population was 76 mutational steps from Perijá population, while in 28S, was 121 mutational steps from W-MV. Uniformly, Perijá was highly divergent from *A. bogotensis s.s.* in the three loci, being 52, 18 and 9 mutational steps in COI, 28S and ITS2 (see Figure 5, Supp. Figure 1).

We recovered W-MV and E-MV groups in haplotype networks with 34, 6 and 1 mutations in between for COI, 28S and ITS2, respectively (see Figure 5, Sup. Figure

1). With an expansion signal on W-MV, consistent with Tajima's D values (see Table 1, Supplementary Table 3). Noting that there are more substitutions between clades on the COI marker than in the nuclear markers, we believe that mtDNA is the primary driver of the phylogenetic signal in our multilocus ML analysis. Nonetheless, in its network, the haplotypes from Tena were 30 and 29 mutational steps from both Bogotá and W-MV group. We did not observe identical shared haplotypes between populations of W-MV and E-MV groups in our loci, nor did we identify shared haplotypes between Tena and Bogotá. However, we found some divergent W-MV haplotypes that were closer to Bogotá haplotypes than to its group, OC_3, OC_34 and OC_229, from three different populations Tenerife, Cali and Manizales (see Figure 5 and Supp. Figure).

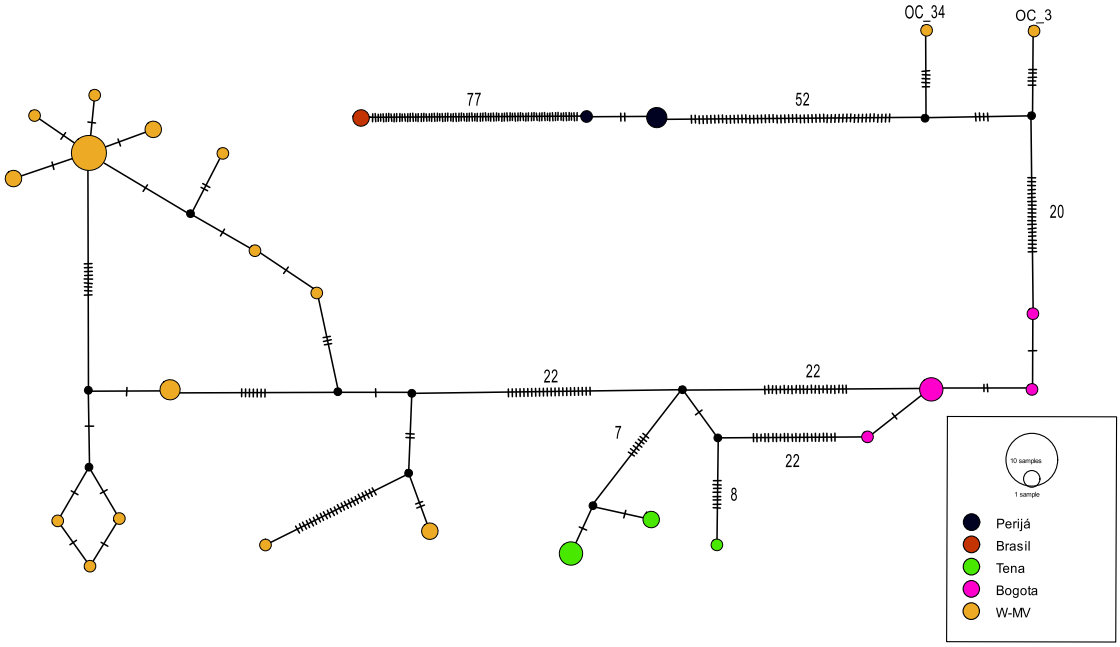

Figure 5: Haplotype network for COI locus. Ticks or numbers on branches represent mutational steps. The size of the circles represents the number of individuals with the same haplotype. Colors represent either populations or genetic clusters.

Consistently with the haplotype networks, population structure statistics (Fst, Dxy and Da) revealed similar patterns of genetic differentiation across loci. Perijá population showed a clear structure pattern from every other population (see Figure 6). Populations from E-MV and W-MV groups showed structure between them (see Figure 6). Moreover, within the E-MV group, Tena and Bogotá showed a considerable genetic differentiation between them (see Figure 6). In contrast, within the W-MV group, populations showed relatively weak genetic differentiation among themselves (see Figure 6). As expected, La Plata, Huila showed weak structure with Tena but also, with W-MV. Hudson test was significant for Fst estimates in nuclear loci (ITS2: Snn: 0.57097, P-value of Snn < 0.0001; 28S: Snn: 0,79293, P-value of Snn < 0,0001).

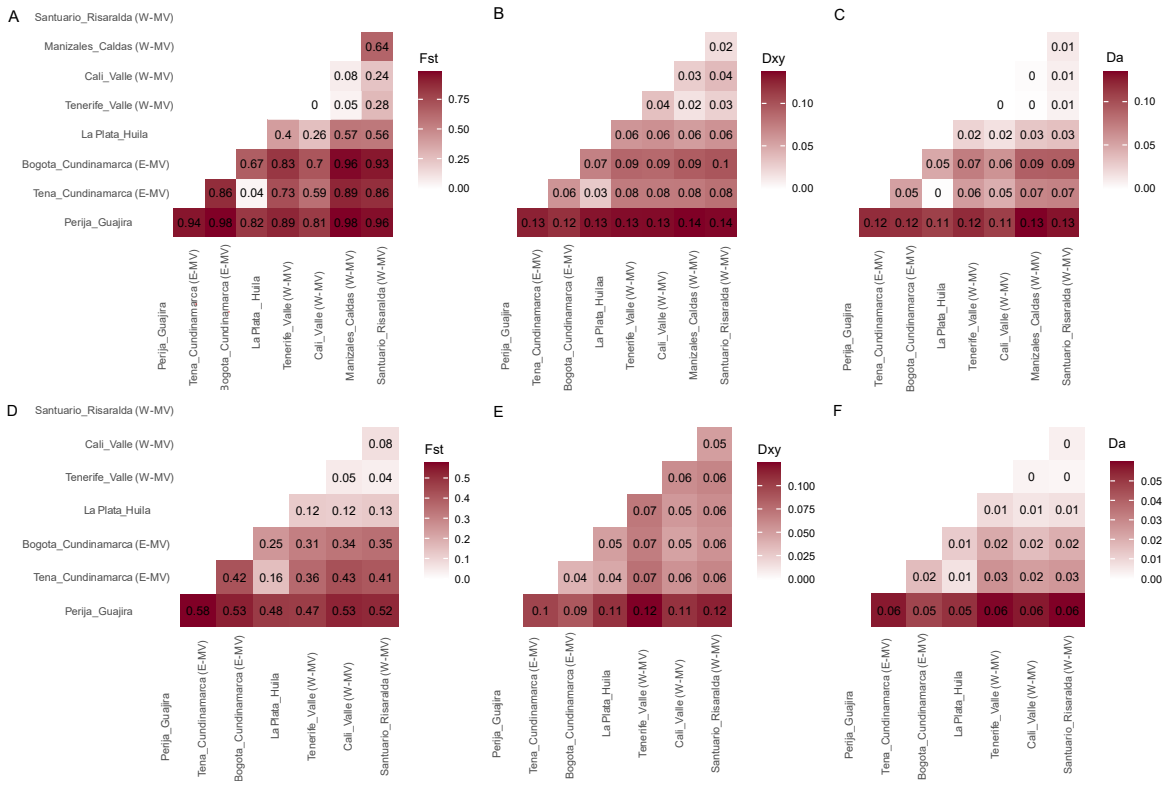

Figure 6: Heatmap illustrating the genetic pairwise differences between populations; Santuario_Risaralda, Cali_Valle and Tenerife_Valle represent the W-MV group, while Bogotá_Cundinamarca and Tena_Cundinamarca correspond to E-MV group. Perijá_Guajira stands alone. Panels A, B and C display the Fst, Dxy and Da measures, respectively, for the COI marker. D, E and F show the same measures for 28S. Genetic pairwise differences for ITS2 marker are shown on Supplementary Figure

Furthermore, genetic variation of this spider clustered in two groups following the Evanno's method (K = 2; see Supp. Figure 2). The first cluster comprises individuals from the W-MV group (green in Figures 3 and 4), while the second cluster includes individuals from the E-MV group as well as the four individuals from Perijá (dark blue in Figures 3 and 4). Recognizing the potential bias associated with different sample

sizes from each region, we also visualized K = 3, where W-MV, E-MV and Perijá appeared as structured regions. However, it is worth noting that some individuals from both E-MV and W-MV groups exhibited shared ancestry. Specifically, within the W-MV group, two individuals displayed more than 50% of shared variation with the other group, not surprisingly, the two individuals that comprise the fourth clade (red asterisks in Figure 7). There were also several individuals in both W-MV and E-MV that presented less than 50% of shared variation, which may represent cases of backcrossing (black asterisks in Figure 7). The possible introgression in these cases ranged from 4% - 45%, with individuals from several population. Since Huila has four individuals closest to the Central Cordillera and another two closest to the East Cordillera (see Figure 1), the first four were grouped with the W-MV and second two were grouped with E-MV, the same two presented in Tena clade in phylogenetic analyses (lower orange asterisks in Figure 7; Figure 4). Noteworthy, two of the ones grouped with W-MV two presented introgression. Interestingly, in K = 3, one individual from Bogotá showed 22% of shared variation with Perijá population. Tena and Bogota fell into the E-MV cluster not having the structured observed in haplotype networks and differentiation indexes (see Figure 5).

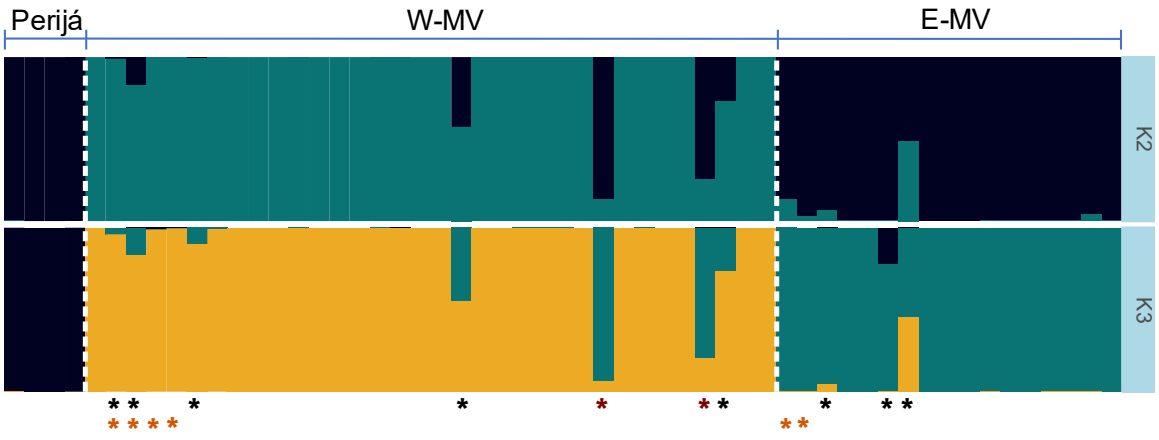

Figure 7: Population assignment test with Structure using the concatenated matrix. The bars represent Bayesian assignment probabilities for each individual to a specific group. In the K = 2 scenario, dark blue represents E-MV and Perijá, while light blue represents W-MV. In K = 3 scenario, dark blue represents Perijá, light blue stands for E-MV, and yellow represents W-MV. The bars at the top indicate the geographic groups. First row of asterisks at the bottom indicates individuals with shared ancestry. Second row of asterisks at the bottom indicate Huila individuals.

Our clustering analysis point to the present of geographic isolated regions, with some individuals sharing ancestry or having genetic flow. IBD analysis showed no statistical significance for the null hypothesis in the three genes (COI: P-value = 0.195, ITS2: P-value = 0.132 and 28S: P-value = 0.291). The analysis of Estimated Effective Migration Surfaces revealed lower-than-average effective migration rates between the A. bogotensis s.s. and Perijá. Also, it revealed a lower-than-average effective migration rates between W-MV and E-MV groups (see Figure 8). The Monmonier´s algorithm barrier test was concordant with Fst and networks patterns, identified the Magdalena River Valley as biogeographical barrier to gene flow between W-MV and E-MV groups in COI, and another barrier between *A. bogotensis s.s.* with Perijá in 28S (see Figure 9). Both barriers were consistent with EEMS results (see Figure 8).

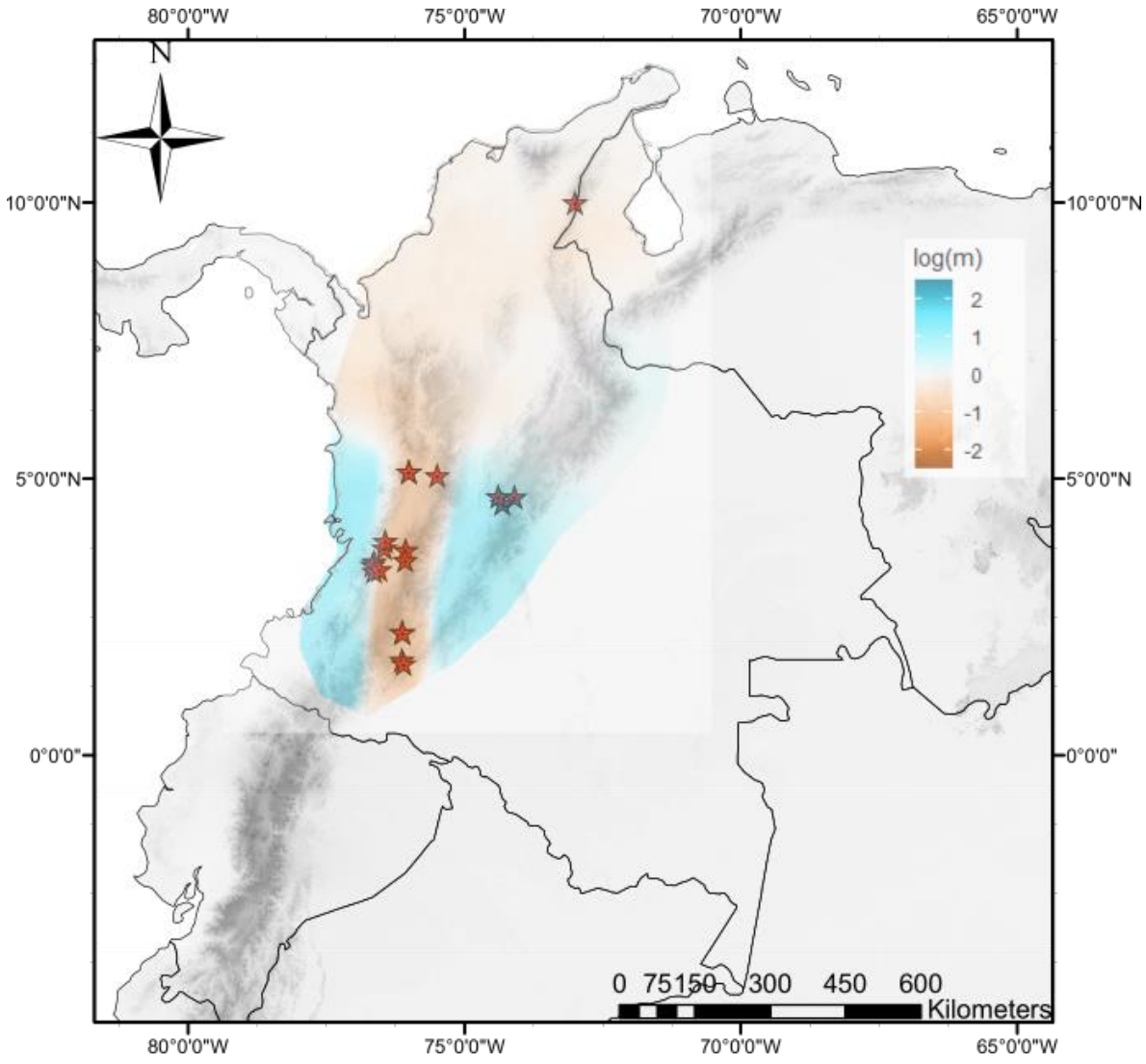

Figure 8: Effective migration patterns from the entire dataset. Higher-than-average and lower-than-average effective migration patterns between different locations are represented with blue and brown colors, respectively.

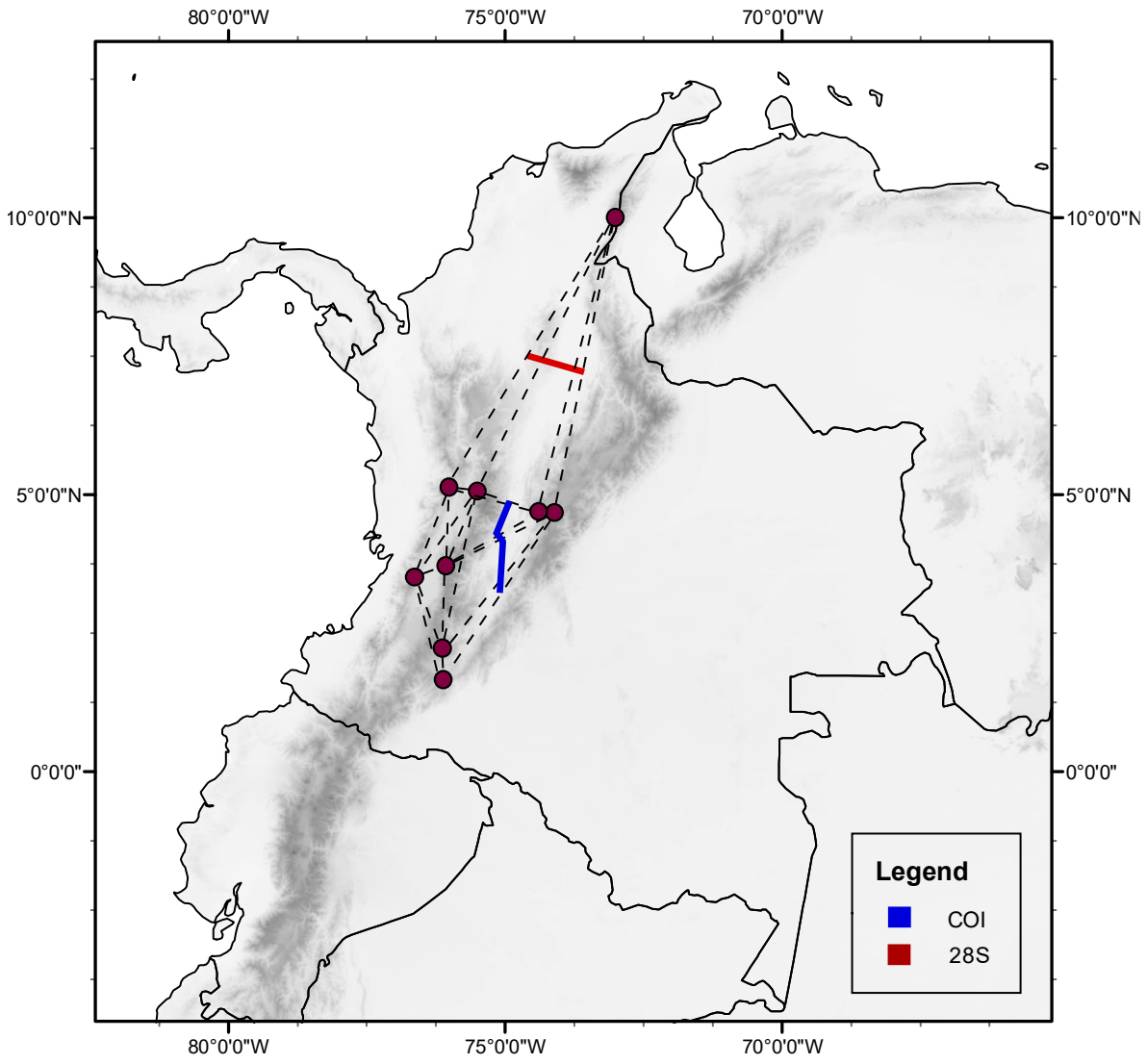

Figure 9: Geographical barrier test based on Monmonier´s algorithm with solid lines representing the main geographic barriers, and dotted lines being the Delaunay triangulation and Voronoi tessellation. The blue and red solid lines are the result of the COI and 28S matrices, respectively.

Demographic model testing

We investigated if the shared ancestry between E-MV and W-MV is due to divergence with gene flow in PHRAPL. The best-fitting model was the one without any gene flow between the two groups. However, this scenario shows some

uncertainty (wAIC = 0.44) as AIC values were not considerable different between models (see Figure 10, Supplementary Table 1). Since Perijá population showed scarce evidence of gene flow or shared ancestry with *A. bogotensis s.s.* we decided not to include it in this analysis.

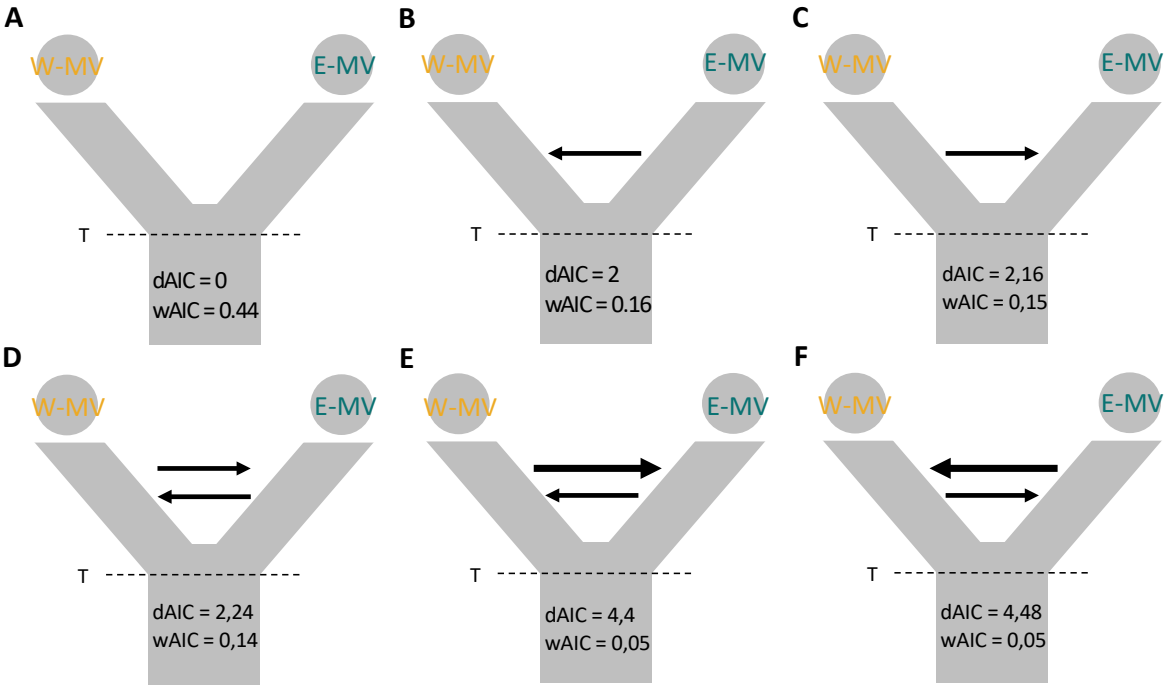

Figure 10: Demographic models used to test the evolution of *A. bogotensis sensu stricto* groups with Phylogeographic Inference Using Approximate Likelihoods (PHRAPL). A, divergence with no migration. B, divergence with unidirectional migration from W-MV group to E-MV group. C, migration with unidirectional migration from E-MV group to W-MV group. D, divergence with bidirectional symmetrical migration. E, divergence with bidirectional asymmetrical migration from W-MV to E-MV group. F, divergence with bidirectional asymmetrical migration from E-MV to W-

MV. Support values from demographic scenarios are shown in each figure. (See Supplementary Table 1).

Species Delimitation

Most of the species accounted for this analysis were not supported as species by iBPP (*A. pentagramicus*, *A. mitificus*, *A. amabilis*, *A. vincibilis*, *A. ishisawi*, *A. variegatus*, *A. stella* and *A. trifolium*; posterior probabilities less than 90; see Figure 11) in most of the tested scenarios. Revisions for species status are required for most *Araneus* spp. here reviewed. Only based in this analysis Brazilian population could be A. vincibils. *Perijá* population showed as a clearly defined *A. blumenau* sister species. Within *A. bogotensis s.s.*, W-MV, Tena population and Bogotá population were recovered as independent lineages with robust support in almost all combinations of priors, having an exception when τ = 2000, indicating a relatively recent divergence (see Figure 11).

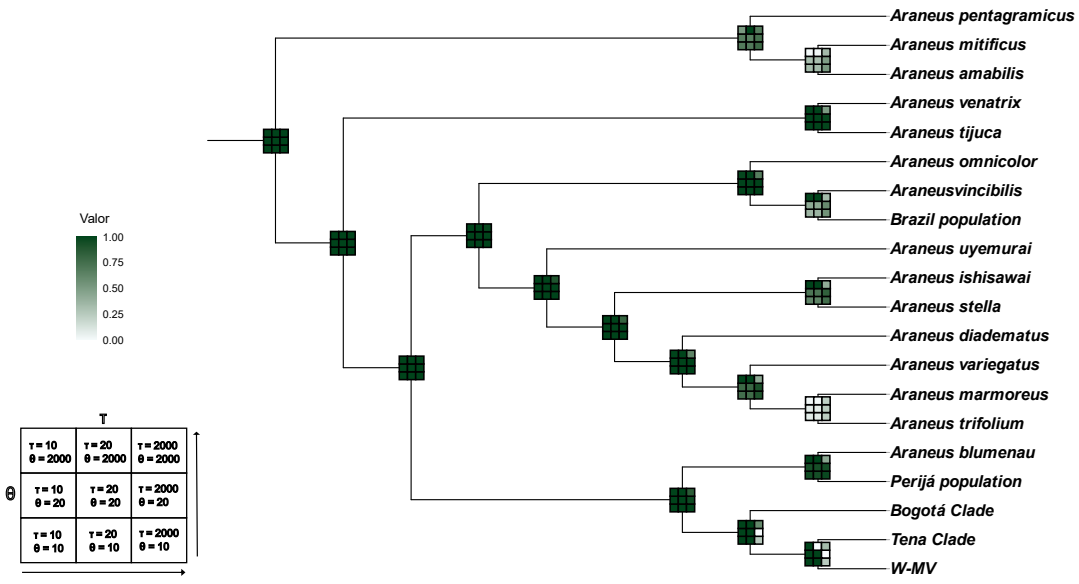

Figure 11: Integrative Bayesian species delimitation with iBPP. Posterior probabilities of 3 x 3 combinations of τ and θ prior distributions are illustrated at each node.

Geometric morphology

In the PCA analysis, the first two principal components accounted for 25.26% and 15.52% of the total variance, respectively (see Figure 12). Notably, the W-MV group, the E-MV group and Perijá population presented statistical differences based on an ANOVA (F = 4.89, P-value = 0.001). Nevertheless, the discriminant analysis (DAPC) successfully recovered distinct clusters for each region with 83.6% of the variance explained on the first component, and 16.4% on the second one (see Figure 13). This suggests that there is some variation in shape, capable of differentiate among the different groups.

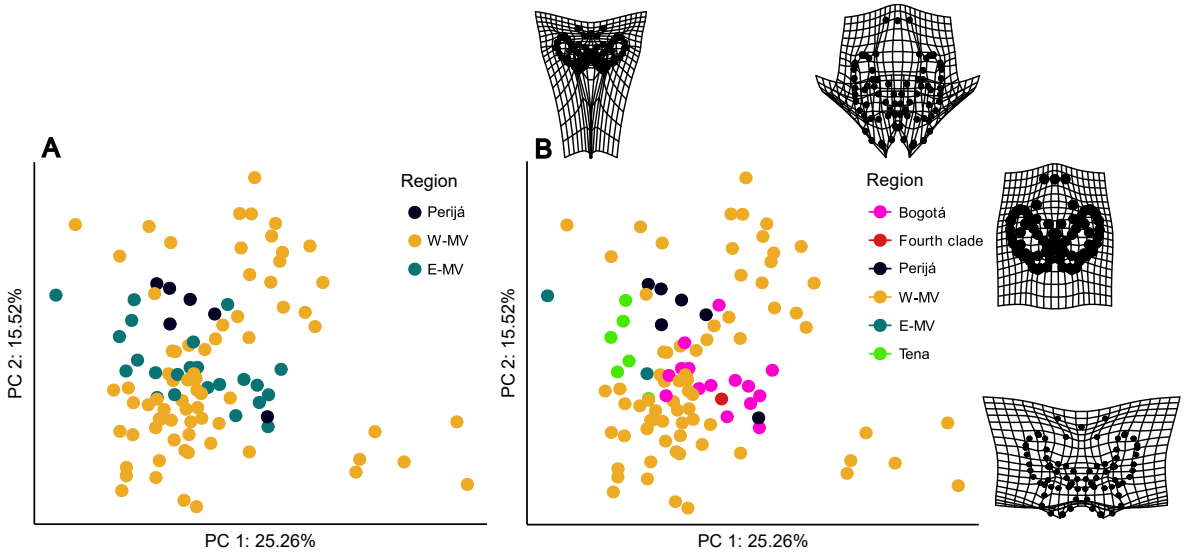

Figure 12: A and B represent PCA colored by regions with W-MV as a whole, and E-MV divided into Tena and Bogotá populations. Deformation plains of each PC showing its maximum and minimums of the epigynum shape in B.

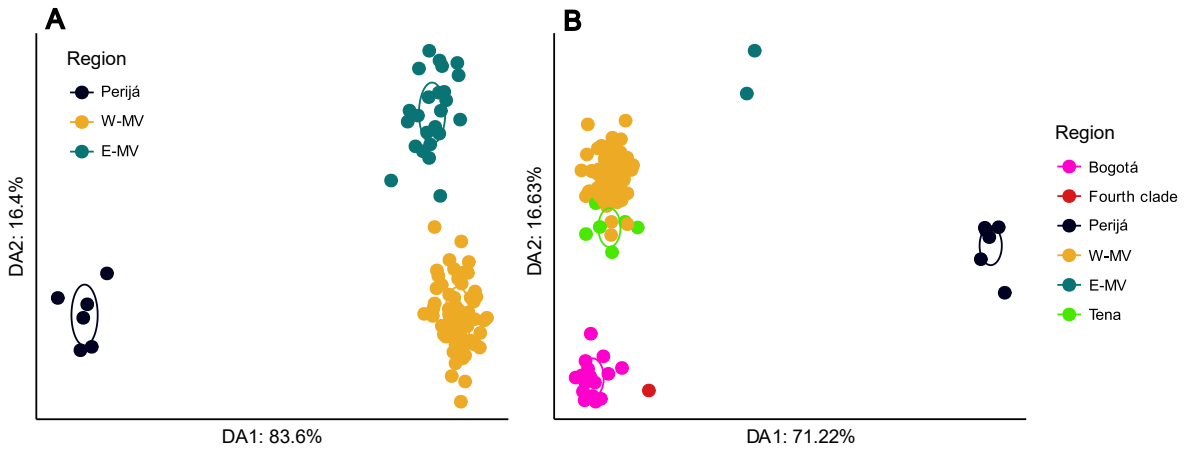

Figure 13: A and B represent DAPC analysis with E-MV as a whole and E-MV divided into Tena and Bogotá, respectively.

To further explore Epigynum morphological variation, we conducted a Model-Based Clustering analysis, which indicates that the best-fitting model has a diagonal distribution, equal volume and equal shape (EEI, BIC = 748.7822). This model clustered the data into three groups, although alternative groupings were possible due to the flat distribution of BIC values (see Figure 14, A). Notably, the EEI clusters did not correspond to the previously described lineages. The first cluster consisted of 18 individuals from the W-MV group, originating from a single population in Palmira, Valle, and one E-MV group individual from Bogotá. The second and larger cluster comprises 53, 23 and 6 individuals from W-MV group, E-MV group and Perijá population, respectively. The third cluster encompasses 6 W-MV group individuals from different populations.

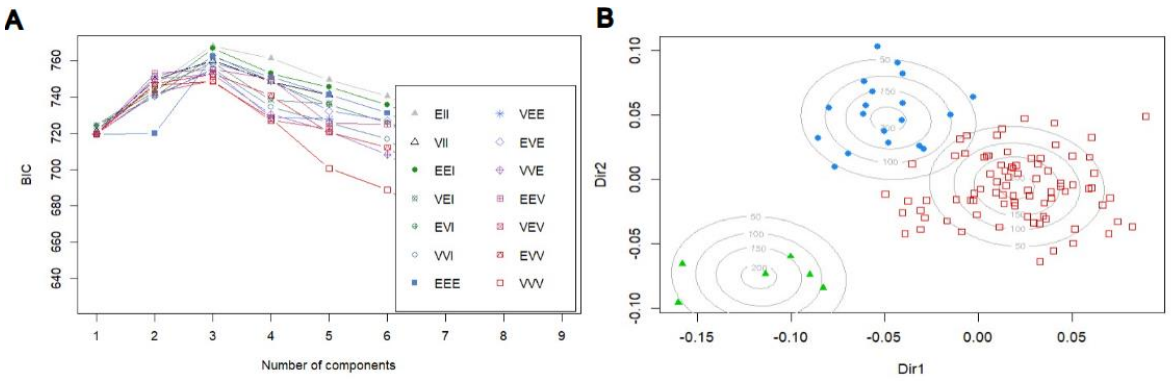

Figure 14: Model-Based Clustering analysis result. A, distribution of the BIC values. B, PCA colored by assign clusters, blue cluster groups 18 individuals from W-MV of a single population named Palmira, red cluster gathers individuals from E-MV, W-MV and Perijá and green cluster groups the 6 inter-mixed samples.

Discussion

Our results are consistent with the complex phylogenetic pattern observed previously for *Araneus* spp. (44). In our main phylogeny we found several clades with Holartic and South American species grouping together forming multiple polyphyletic species. Further efforts with more sampling of loci and populations could be required to resolve the *Araneus* phylogeny. Inside what is called by taxonomists *Araneus bogotensis*, using genetics and morphology, we found that there were three divergent independent clades that may correspond to three different cryptic species, the Brazilian population, the Perijá population and what we named as *Araneus bogotensis sensu stricto*. This issue might have several causes, for example, incomplete or erroneous information about the sequences on Genbank, where researchers sometimes give few or zero details about how and where the samples

were collected (91), out-of-date and unreviewed dichotomous keys based on labile traits, and the one that probably contributes the most, the lack of research studies in Neotropics' spiders (92).

The Brazilian and Perijá populations showed an estimated divergence time from *A. bogotensis s.s*. of 18.47 Mya and 10.9 Mya, respectively (see Figure 4). The first coinciding with Early-Mid Miocene where high temperatures and aridity dominated most landscapes worldwide (8). At that time, Northern Andes had its first mountain building peak (~23 Mya) (8) so we hypothesize the MRCA between the Brazilian populations and *A. bogotensis s.s.* lived somewhere close to Central Andes, and from there the species started dispersing to Northern Andes as it gained altitude and Southern Brazil. On the other hand, the divergence time of the MRCA between Perijá population, its sister species *A. blumenau*, and *A. bogotensis s.s.* was around Late Miocene, in the middle of the last and most intense peak of mountain building in the Northern Andes (~12 Mya) (8). This suggest four possible scenarios assuming *A. blumenau* has been correctly identified in the related studies, one with a vicariant event in which the lowlands aridity stopped the dispersal on the species as soon as Serranía del Perijá reached for higher altitudes (93), another one in which the intense uplift of the Andes generated distinct habitats that might have caused local adaptations on both sides and generated further diversification (94), a third one in which the Perijá population could have been introduced to that place, since it has a Brazilian species as sister, from which we know it has a faraway distribution from Southern Brazil to Northern Argentina (53), and a last one, in which the geomorphology of the Andes was not a substantial factor affecting the divergence

between *A. bogotensis s.s.*, Perija population and *A. blumenau*, and the MRCA of the latter two may have shared the current distribution of *A. bogotensis s.s.*. For those reasons, more information about the natural history of *A.blumenau* would be crucial to understand this diversification pattern.

Another important divergence observed in this study was between lineages within *A. bogotensis s.s.* where its phylogenetic relationships might have been influenced by the Andes topography. We identified divergence between the west and east populations of the Magdalena River Valley (W-MV and E-MV; see Figures 7, 8, 9), suggesting a vicariant event. We hypothesize that the Magdalena River Valley is acting as a strong barrier to gene flow for this species since we did not detect a clear pattern of introgression among east and west groups, consistent with PHRAPL's No Gene Flow best fitting model result. Vicariant events produced by Andes Mountains and Valleys have been observed for many taxa including birds (11,19), amphibians (95), spiders (96,97) and beetles (73). The estimated divergence time, between W-MV and E-MV (Tena clade), happened 3.65 Mya at the ending of the final uplift of Northern Andes when the Eastern cordillera and the Magdalena Valley were formed, 3 – 17 Mya reinforcing the vicariance hypothesis (98). In addition, we do not have studies about this spider's natural history traits, ecology and physiology. For example, we do not know if *A. bogotensis* can do ballooning, despite the fact that researchers have reported this behavior in spiders of the same family (23,99). This ability could augment their dispersal capabilities.

It is noteworthy that in Huila, the only population where we observed shared ancestry in more than one individual, we found also individuals from both W-MV and E-MV

groups coexisting in sympatry in this region (see Figure 7). This can be explained since there is no physical barrier at that place, being located in the middle of the two cordilleras and before the beginning of the Magdalena River Valley. This population can be a relict of the genetic variation that is now sorted in the W-MV and E-MV groups and also is consistent with a possible dispersion event from the south to the north coupled with vicariance caused by the Magdalena valley. The drivers for spider's diversification a both sides of the Magdalena valley are not known but we hypothesize it had to be related to historical drastic environmental conditions and/or not suitable habitat for this spiders inside the valley. Additionally, local adaptation through natural selection of these two lineages might have taken the diversification further (94,100). Future studies should focus on assessing if reproductive isolation exist between the members of these two groups (W-MV and E-MV) and increasing the number of loci and the number of populations on the E-MV to gain quantitative information on how divergent those groups really are, and which of the theories, if vicariant or dispersal, are more consistent with data. Additionally, experimental confirmation of their capacity to interbreed would help to clear a picture of the level of reproductive isolation the populations are having in Huila.

Beyond that, the two populations from E-MV group, Tena and Bogotá, also showed signs of structure from one another in haplotype networks, differentiation indexes and morphometric analysis (see Figures 5, 6, 12, 13). A pattern consistent with the phylogenies, which resulted in an estimated divergence time between Bogotá and Tena+W-MV of 4.95 Mya (see Figure 4. We believe that Bogotá population might represent a very old lineage or a different species from *A. bogotensis*. Despite their

relative proximity, the two locations present very different ecosystems, for example, Tena is warmer with a mean altitude of 1384 m, meanwhile Bogotá has a colder mean temperature with a mean altitude of 2557 m. These differences may have caused deep divergence through time due to a divergent local adaptation (94) and may represent a barrier to gene flow in the present. Furthermore, Tena is closer to W-MV which may allowed more genetic flow between those populations in the past. We recognize that sampling biases due to few loci (101,102), little number of per population specimens (76,103) and a close proximity (83) to Tena could have grouped them together in various analyses. Further investigations in this matter will need to increase the number of populations sampled to the east of the Magdalena River Valley.

Lastly, we hypothesized that the divergent Fourth clade is a different species from *A. bogotensis* and possibly a different species from the Bogotá population. The morphotype for 34_BosquedeNieblaSanAntonio_Cali individual (red square in Figure 1) and the phylogenetic and haplotype divergence (see Figures 3, 4, 5) made it a clearly different species candidate. We believe that the position of this clade in the topologies obtained is merely an artefact of the few sequences available.

This study represents a first attempt to describe the phylogenetics of one of the putative *Araneus* spp. present in Colombia and one of the few, to address this issue in the Neotropics. We demonstrated the existence of three divergent independent cryptic lineages from what is called *Araneus bogotensis* that need a detailed taxonomic review, the Brazil population, the Perijá population and *A. bogotensis s.s.*. Additionally, we hypothesized two more candidate new species, the Bogotá

population and the Fourth clade. Further studies should focus on increasing the populations sampling at the east of the Magdalena River Valley as well as to explore the drivers of the speciation in Huila populations.

Supplementary Figures

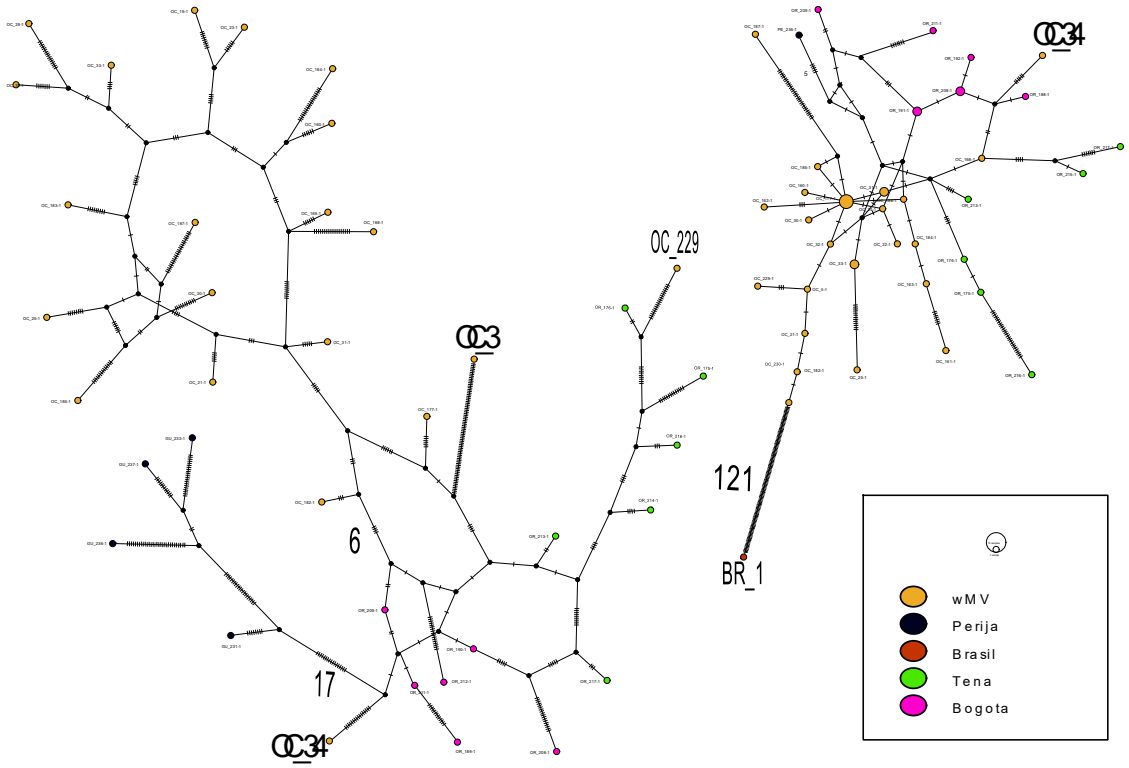

Supplementary Figure 1: 28S and ITS2 haplotypic networks.

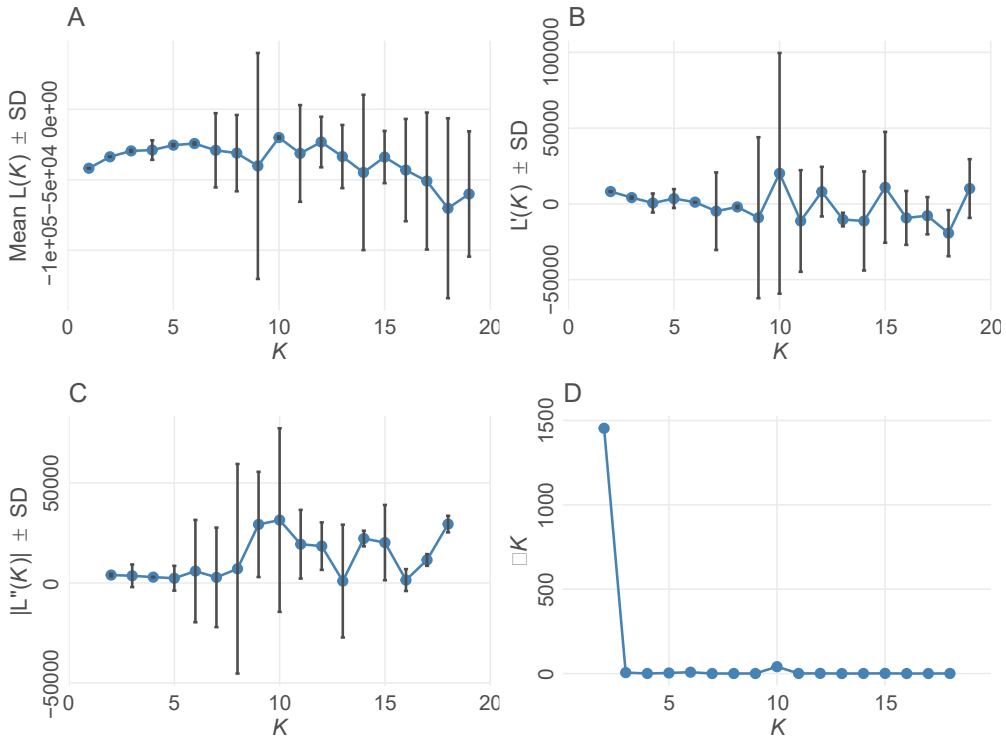

Supplementary figure 5: Evanno summary statistics. A, estimated ln probability of data plus standard deviation. B, first derivate plus standard deviation. C, second derivative plus standard deviation. D, delta K.

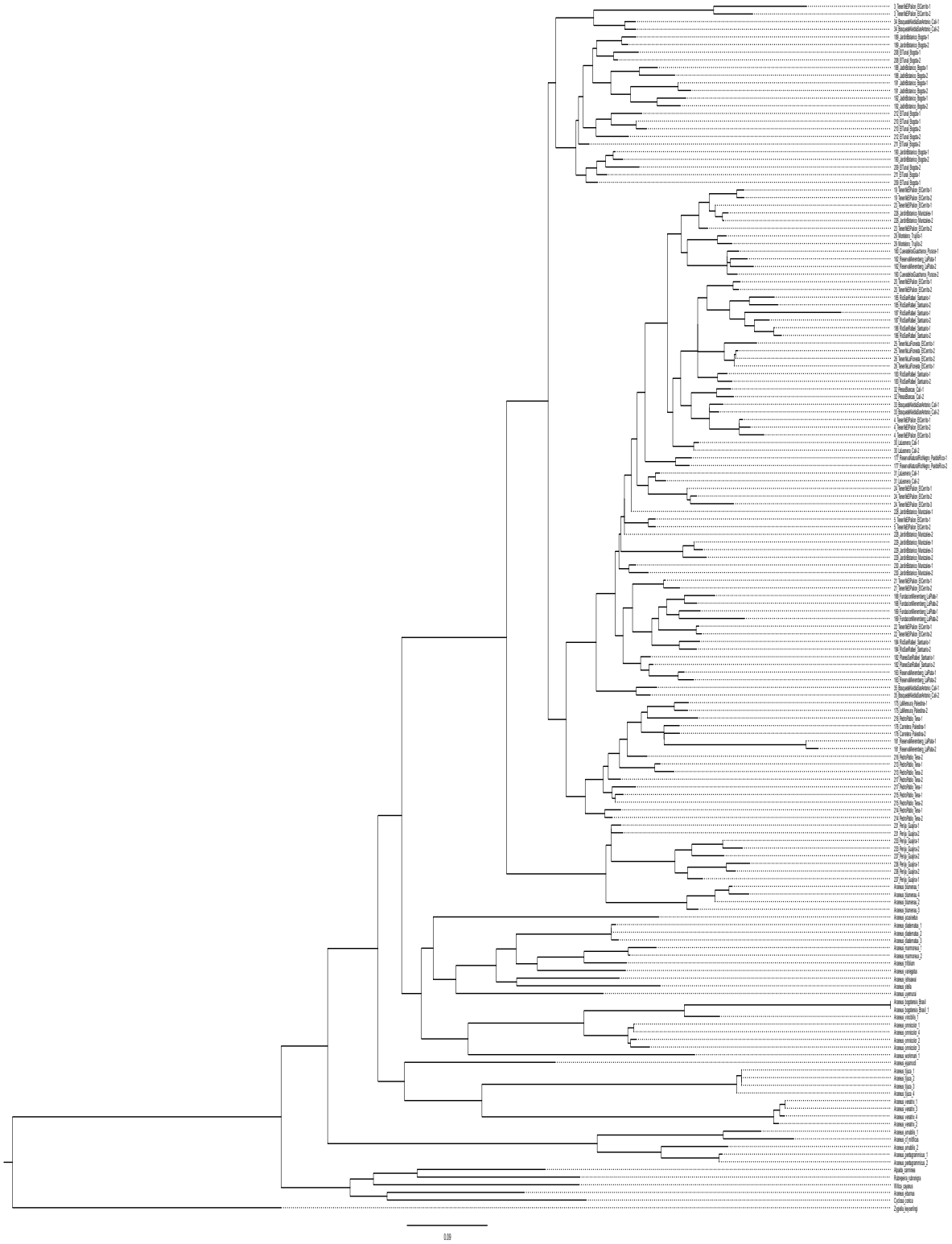

Supplementary Figure 6: Maximum likelihood topology with all branches.

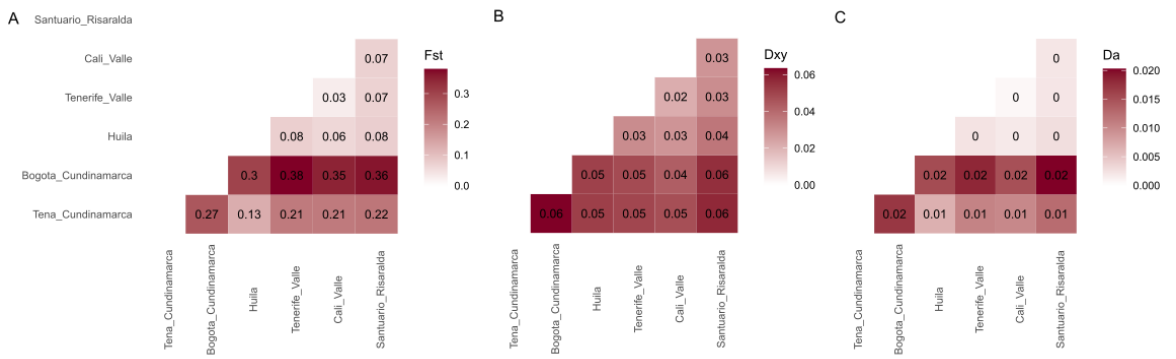

Supplementary Figure 7. Genetic pairwise differences for ITS2 marker. A, B and C show Fst, Dxy and Da indexes respectively.

Models	AIC	dAIC	wAIC
1	139.462322197575	0	0.444297387659864
2	141.462322197575	2	0.163447874686242
3	141.622722197575	2.16	0.150881404905025
4	141.702922197575	2.241	0.144892795884653
5	143.863322197575	4.401	0.0492049451806135
6	143.943522197575	4.481	0.0472755916836024

Supplementary Table 1: PHRAPL: AIC, dAIC and wAIC estimates for the six models evaluated.

Primer	Sequence
LCO1490	5'-GGTCAACAAATCATAAAGATATTGG-3'
HCO2198	5'-TAAACTTCAGGGTGACCAAAAAATCA-3'
5.8	5'-GCTGCGTTCTTCATCGATGC-3'
28S	5'-GGTCCGTGTTTCAAGACGG-3'

28SO	5'-GAAACTGCTCAAAGGTAAACGG-3'
28SC	5'-GGTTCGATTAGTCTTTCGCC-3'
27F	5'-AGAGTTTGATCCTGGCTCAG-3'
1492R	5'-GGTTACCTTGTTACGACTT-3'

Supplementary Table 2: Primers.

	COI					ITS2					28S				
Clade	W-MV	Tena	Bogotá	Cuarto	Perija	W-MV	Tena	Bogotá	Fourth	Perija	W-MV	Tena	Bogotá	Fourth	Perija
N	15	7	7	2	4	59	12	16	2	2	38	12	12	4	8
#H	14	3	4	2	2	38	12	15	2	2	38	12	12	4	8
Hd	0,88	0,667	0,714	1	0,5	0,96	1	0,992	1	1	1	1	1	1	1
pi	0,016	0,011	0,003	0,028	0,002	0,022	0,056	0,041	0,012	0,016	0,051	0,03	0,029	0,093	0,059
Theta	0,022	0,015	0,003	0,028	0,002	0,068	0,07	0,059	0,025	0,016	0,062	0,03	0,033	0,09	0,055
SS	40	18	4	14	2	76	58	62	13	5	166	61	71	110	88
Tajima´s D	-1,04	-1,31	-0,32		-0,71	-2,34	-0,92	-1,27			-0,65	-0,01	-0,61	0,31	0,36
Fu and Li's D	-1,67	-1,4	-0,07	0	-0,71	-3,86	-0,97	-1,35	0	0	-0,25	0,29	-0,02		0,57

Supplementary Table 3: Population genetic summary statistics from clades for each locus. N: number of sequences, Hd: haplotype diversity, pi: nucleotide diversity per site, theta: expected nucleotide diversity per site, SS: segregating sites. Highlighted values are statistically significant with P-value < 0.05.

Bibliography

1. Kim KC, Byrne LB. Biodiversity loss and the taxonomic bottleneck: emerging biodiversity science. Ecol Res. 2006 Nov 1;21(6):794–810.

2. Schlick-Steiner BC, Steiner FM, Seifert B, Stauffer C, Christian E, Crozier RH. Integrative Taxonomy: A Multisource Approach to Exploring Biodiversity. Annu Rev Entomol. 2010;55(1):421–38.

3. Raupach MJ, Amann R, Wheeler QD, Roos C. The application of "-omics" technologies for the classification and identification of animals. Org Divers Evol. 2016 Mar 1;16(1):1–12.

4. Bickford D, Lohman DJ, Sodhi NS, Ng PKL, Meier R, Winker K, et al. Cryptic species as a window on diversity and conservation. Trends Ecol Evol. 2007 Mar;22(3):148–55.

5. Stern DL. The genetic causes of convergent evolution. Nat Rev Genet. 2013 Nov;14(11):751–64.

6. Pfenninger M, Schwenk K. Cryptic animal species are homogeneously distributed among taxa and biogeographical regions. BMC Evol Biol. 2007 Jul 19;7(1):121.

7. Nelson G, Platnick N. Systematics and Biogeography. Harcourt, Brace and World; 1981.

8. Hoorn C, Wesselingh FP, ter Steege H, Bermudez MA, Mora A, Sevink J, et al. Amazonia through time: Andean uplift, climate change, landscape evolution, and biodiversity. Science. 2010 Nov 12;330(6006):927–31.

9. Boschman LM, Condamine FL. Mountain radiations are not only rapid and recent: Ancient diversification of South American frog and lizard families related to Paleogene Andean orogeny and Cenozoic climate variations. Glob Planet Change. 2022 Jan 1;208:103704.

10. Dick CW, Roubik DW, Gruber KF, Bermingham E. Long-distance gene flow and cross-Andean dispersal of lowland rainforest bees (Apidae: Euglossini) revealed by comparative mitochondrial DNA phylogeography. Mol Ecol. 2004;13(12):3775–85.

11. Hazzi NA, Moreno JS, Ortiz-Movliav C, Palacio RD. Biogeographic regions and events of isolation and diversification of the endemic biota of the tropical Andes. Proc Natl Acad Sci. 2018 Jul 31;115(31):7985–90.

12. Hutter CR, Lambert SM, Wiens JJ. Rapid Diversification and Time Explain Amphibian Richness at Different Scales in the Tropical Andes, Earth's Most Biodiverse Hotspot. Am Nat. 2017 Dec;190(6):828–43.

13. Patterson BD. ON DRIVERS OF NEOTROPICAL MAMMAL DIVERSIFICATION. Mastozool Neotropical. 2020;27:15–26.

14. Antonelli A, Quijada A, Crawford A, Bates J, Velazco P, Wüster W. Amazonia: Landscape and Species Evolution: A look into the past. In 2010. p. 386–404.

15. Smith BT, McCormack JE, Cuervo AM, Hickerson MJ, Aleixo A, Cadena CD, et al. The drivers of tropical speciation. Nature. 2014 Nov;515(7527):406–9.

16. Ayres JM, Clutton-Brock TH. River Boundaries and Species Range Size in Amazonian Primates. Am Nat. 1992 Sep;140(3):531–7.

17. Hayes FE, Sewlal JAN. The Amazon River as a dispersal barrier to passerine birds: effects of river width, habitat and taxonomy. J Biogeogr. 2004;31(11):1809–18.

18. Pulido-Santacruz P, Aleixo A, Weir JT. Morphologically cryptic Amazonian bird species pairs exhibit strong postzygotic reproductive isolation. Proc R Soc B Biol Sci. 2018 Mar 7;285(1874):20172081.

19. Gutiérrez-Pinto N, Cuervo AM, Miranda J, Pérez-Emán JL, Brumfield RT, Cadena CD. Non-monophyly and deep genetic differentiation across low-elevation barriers in a Neotropical montane bird (Basileuterus tristriatus; Aves: Parulidae). Mol Phylogenet Evol. 2012 Jul 1;64(1):156–65.

20. Link A, Valencia LM, Céspedes LN, Duque LD, Cadena CD, Di Fiore A. Phylogeography of the Critically Endangered Brown Spider Monkey (Ateles hybridus): Testing the Riverine Barrier Hypothesis. Int J Primatol. 2015 Jun 1;36(3):530–47.

21. Sandoval-H J, Gómez JP, Cadena CD. Is the largest river valley west of the Andes a driver of diversification in Neotropical lowland birds? The Auk. 2017 Jan 1;134(1):168–80.

22. Solomon SE, Jr MB, Jr JM, Vinha GG, Mueller UG. Paleodistributions and Comparative Molecular Phylogeography of Leafcutter Ants (Atta spp.) Provide New Insight into the Origins of Amazonian Diversity. PLOS ONE. 2008 Jul 23;3(7):e2738.

23. Bell JR, Bohan DA, Shaw EM, Weyman GS. Ballooning dispersal using silk: world fauna, phylogenies, genetics and models. Bull Entomol Res. 2005 Apr;95(2):69–114.

24. Beheregaray LB, Caccone A. Cryptic biodiversity in a changing world. J Biol. 2007;6(4):9.

25. Huber BA. Sexual selection research on spiders: progress and biases. Biol Rev. 2005 Aug;80(3):363–85.

26. Foelix R. Biology of Spiders [Internet]. Vol. 3rd ed. New York: Oxford University Press; 2011 [cited 2023 Aug 21]. Available from: http://ez.urosario.edu.co/login?url=https://search.ebscohost.com/login.aspx?direct=true&AuthType=ip&db=e000xww&AN=348160&lang=es&site=eds-live&scope=site

27. Agnarsson I, LeQuier SM, Kuntner M, Cheng RC, Coddington JA, Binford G. Phylogeography of a good Caribbean disperser: Argiope argentata (Araneae, Araneidae) and a new 'cryptic' species from Cuba. ZooKeys. 2016 Oct 19;(625):25–44.

28. Dupérré N. Description of the first visually cryptic species of Paratropis (Araneae: Paratropididae) from Ecuador. J Arachnol. 2015 Nov;43(3):327–30.

29. Hamilton CA, Formanowicz DR, Bond JE. Species Delimitation and Phylogeography of Aphonopelma hentzi (Araneae, Mygalomorphae, Theraphosidae): Cryptic Diversity in North American Tarantulas. PLOS ONE. 2011 Oct 12;6(10):e26207.

30. Hendrixson BE, Bond JE. Testing species boundaries in the Antrodiaetus unicolor complex (Araneae: Mygalomorphae: Antrodiaetidae): "Paraphyly" and cryptic diversity. Mol Phylogenet Evol. 2005 Aug 1;36(2):405–16.

31. Leavitt DH, Starrett J, Westphal MF, Hedin M. Multilocus sequence data reveal dozens of putative cryptic species in a radiation of endemic Californian mygalomorph spiders (Araneae, Mygalomorphae, Nemesiidae). Mol Phylogenet Evol. 2015 Oct 1;91:56–67.

32. Oh JH, Kim S, Lee S. DNA barcodes reveal population-dependent cryptic diversity and various cases of sympatry of Korean leptonetid spiders (Araneae: Leptonetidae). Sci Rep. 2022 Sep 15;12(1):15528.

33. ŘEzáč M, Pekár S, Johannesen J. Taxonomic review and phylogenetic analysis of central European Eresus species (Araneae: Eresidae). Zool Scr. 2008;37(3):263–87.

34. Starrett J, Hedin M. Multilocus genealogies reveal multiple cryptic species and biogeographical complexity in the California turret spider Antrodiaetus riversi (Mygalomorphae, Antrodiaetidae). Mol Ecol. 2007;16(3):583–604.

35. Gloor D, Nentwig W, Blick T, Kropf C. World Spider Catalog. 2017 [cited 2024 Feb 8]; Available from: http://wsc.nmbe.ch

36. Kuntner M, Coddington JA, Hormiga G. Phylogeny of extant nephilid orb-weaving spiders (Araneae, Nephilidae): testing morphological and ethological homologies. Cladistics. 2008;24(2):147–217.

37. Kuntner M, Arnedo MA, Trontelj P, Lokovšek T, Agnarsson I. A molecular phylogeny of nephilid spiders: Evolutionary history of a model lineage. Mol Phylogenet Evol. 2013 Dec 1;69(3):961–79.

38. Chamberland L, Salgado-Roa FC, Basco A, Crastz-Flores A, Binford GJ, Agnarsson I. Phylogeography of the widespread Caribbean spiny orb weaver Gasteracantha cancriformis. PeerJ. 2020 Apr 30;8:e8976.

39. Salgado-Roa FC, Pardo-Diaz C, Lasso E, Arias CF, Solferini VN, Salazar C. Gene flow and Andean uplift shape the diversification of Gasteracantha cancriformis (Araneae: Araneidae) in Northern South America. Ecol Evol. 2018;8(14):7131–42.

40. Williams SH. A phylogeny of the genus Gasteracantha Sundevall, 1833 (Araneae, Araneidae) with an examination of sexually dimorphic characters in the subfamily Gasteracanthinae [Internet] [Ph.D.]. Oxford Brookes University; 2022 [cited 2023 Aug 21]. Available from: https://doi.org/10.24384/h764-wb36

41. Magalhaes ILF, Martins PH, Faleiro BT, Vidigal THDA, Santos FR, Carvalho LS, et al. Complete phylogeny of Micrathena spiders suggests multiple dispersal events among Neotropical rainforests, islands, and landmasses, and indicates Andean orogeny promotes speciation [Internet]. bioRxiv; 2023 [cited 2024 Jan 5]. p. 2023.11.01.565210. Available from: https://www.biorxiv.org/content/10.1101/2023.11.01.565210v1

42. Magalhaes ILF, Santos AJ. Phylogenetic analysis of Micrathena and Chaetacis spiders (Araneae: Araneidae) reveals multiple origins of extreme sexual size dimorphism and long abdominal spines. Zool J Linn Soc. 2012 Sep 1;166(1):14–53.

43. Shapiro L, Binford GJ, Agnarsson I. Single-Island Endemism despite Repeated Dispersal in Caribbean Micrathena (Araneae: Araneidae): An Updated Phylogeographic Analysis. Diversity. 2022 Feb;14(2):128.

44. Scharff N, Coddington JA, Blackledge TA, Agnarsson I, Framenau VW, Szűts T, et al. Phylogeny of the orb-weaving spider family Araneidae (Araneae: Araneoidea). Cladistics Int J Willi Hennig Soc. 2020 Feb;36(1):1–21.

45. Dimitrov D, Benavides LR, Arnedo MA, Giribet G, Griswold CE, Scharff N, et al. Rounding up the usual suspects: a standard target-gene approach for resolving the interfamilial phylogenetic relationships of ecribellate orb-weaving spiders with a new family-rank classification (Araneae, Araneoidea). Cladistics. 2017;33(3):221–50.

46. Kallal RJ, Dimitrov D, Arnedo MA, Giribet G, Hormiga G. Monophyly, Taxon Sampling, and the Nature of Ranks in the Classification of Orb-Weaving Spiders (Araneae: Araneoidea). Syst Biol. 2020 Mar 1;69(2):401–11.

47. Kim JA, Jeon HS, Kang TH, Yoo JS, Jun J. Complete mitogenomes of two orb-weaver spiders, Argiope bruennichi and Araneus ventricosus. Mitochondrial DNA Part B. 2020 Apr 2;5(2):1506–7.

48. Kono N, Nakamura H, Ohtoshi R, Moran DAP, Shinohara A, Yoshida Y, et al. Orb-weaving spider Araneus ventricosus genome elucidates the spidroin gene catalogue. Sci Rep. 2019 Jun 10;9(1):8380.

49. Wang ZL, Li C, Fang WY, Yu XP. The complete mitochondrial genome of orb-weaving spider Araneus ventricosus (Araneae: Araneidae). Mitochondrial DNA Part A. 2016 May 3;27(3):1926–7.

50. Wang ZL, Wang ZY, Huang J, Yu XP. The complete mitochondrial genome of an orb-weaver spider Araneus angulatus (Araneae: Araneidae). Mitochondrial DNA Part B. 2019 Jul 3;4(2):3870–1.

51. Peres EA, Sobral-Souza T, Perez MF, Bonatelli IAS, Silva DP, Silva MJ, et al. Pleistocene Niche Stability and Lineage Diversification in the Subtropical Spider Araneus omnicolor (Araneidae). PLOS ONE. 2015 Apr 9;10(4):e0121543.

52. Peres EA, Silva MJ, Solferini VN. Phylogeography of the spider Araneus venatrix (Araneidae) suggests past connections between Amazon and Atlantic rainforests. Biol J Linn Soc. 2017 Aug 1;121(4):771–85.

53. Levi HW. The Neotropical and Mexican species of the orb-weaver genera Araneua, Dubiepeira, and Aculepeira (Araneae: Araneidae) [Internet]. 1991 [cited 2023 Jun 13]. 149 p. Available from: http://archive.org/details/biostor-620

54. Folmer O, Black M, Hoeh W, Lutz R, Vrijenhoek R. DNA primers for amplification of mitochondrial cytochrome c oxidase subunit I from diverse metazoan invertebrates. Mol Mar Biol Biotechnol. 1994 Oct;3(5):294–9.

55. White T, Bruns T, Lee S, Taylor J, Innis M, Gelfand D, et al. Amplification and Direct Sequencing of Fungal Ribosomal RNA Genes for Phylogenetics. In: Pcr Protocols: a Guide to Methods and Applications,. 1990. p. 315–22.

56. Hedin MC, Maddison WP. A Combined Molecular Approach to Phylogeny of the Jumping Spider Subfamily Dendryphantinae (Araneae: Salticidae). Mol Phylogenet Evol. 2001 Mar 1;18(3):386–403.

57. Stephens M, Smith NJ, Donnelly P. A new statistical method for haplotype reconstruction from population data. Am J Hum Genet. 2001 Apr;68(4):978–89.

58. Rozas J, Ferrer-Mata A, Sánchez-DelBarrio JC, Guirao-Rico S, Librado P, Ramos-Onsins SE, et al. DnaSP 6: DNA Sequence Polymorphism Analysis of Large Data Sets. Mol Biol Evol. 2017 Dec 1;34(12):3299–302.

59. De Coster W, D'Hert S, Schultz DT, Cruts M, Van Broeckhoven C. NanoPack: visualizing and processing long-read sequencing data. Bioinformatics. 2018 Aug 1;34(15):2666–9.

60. Sahlin K, Medvedev P. De novo clustering of long-read transcriptome data using a greedy, quality-value based algorithm [Internet]. bioRxiv; 2018 [cited 2023 Jul 28]. p. 463463. Available from: https://www.biorxiv.org/content/10.1101/463463v1

61. Larsson A. AliView: a fast and lightweight alignment viewer and editor for large datasets. Bioinformatics. 2014 Nov 15;30(22):3276–8.

62. Tamura K, Stecher G, Kumar S. MEGA11: Molecular Evolutionary Genetics Analysis Version 11. Mol Biol Evol. 2021 Jul 1;38(7):3022–7.

63. Nguyen LT, Schmidt HA, von Haeseler A, Minh BQ. IQ-TREE: A Fast and Effective Stochastic Algorithm for Estimating Maximum-Likelihood Phylogenies. Mol Biol Evol. 2015 Jan 1;32(1):268–74.

64. Drummond AJ, Suchard MA, Xie D, Rambaut A. Bayesian Phylogenetics with BEAUti and the BEAST 1.7. Mol Biol Evol. 2012 Aug 1;29(8):1969–73.

65. Kück P, Longo GC. FASconCAT-G: extensive functions for multiple sequence alignment preparations concerning phylogenetic studies. Front Zool. 2014 Nov 18;11(1):81.

66. Fourment M, Darling AE. Local and relaxed clocks: the best of both worlds. PeerJ. 2018 Jul 3;6:e5140.

67. Bartoleti LF de M, Peres EA, Sobral-Souza T, Fontes F von HM, Silva MJ da, Solferini VN. Phylogeography of the dry vegetation endemic species Nephila sexpunctata (Araneae: Araneidae) suggests recent expansion of the Neotropical Dry Diagonal. J Biogeogr. 2017;44(9):2007–20.

68. Bidegaray-Batista L, Arnedo MA. Gone with the plate: the opening of the Western Mediterranean basin drove the diversification of ground-dweller spiders. BMC Evol Biol. 2011 Oct 31;11(1):317.

69. Rambaut A, Drummond AJ, Xie D, Baele G, Suchard MA. Posterior Summarization in Bayesian Phylogenetics Using Tracer 1.7. Syst Biol. 2018 Sep 1;67(5):901–4.

70. Solís-Lemus C, Knowles LL, Ané C. Bayesian species delimitation combining multiple genes and traits in a unified framework. Evolution. 2015;69(2):492–507.

71. Arias-Cárdenas A, Barrientos LS, Pardo-Diaz C, Paz A, Crawford AJ, Salazar C. Taxonomic inflation and a reconsideration of speciation in the Andes: the case of the high-elevation tree frog Dendropsophus molitor (Anura: Hylidae). Zool J Linn Soc. 2023 Sep 16;zlad085.

72. Eberle J, Warnock RCM, Ahrens D. Bayesian species delimitation in Pleophylla chafers (Coleoptera) – the importance of prior choice and morphology. BMC Evol Biol. 2016 May 5;16(1):94.

73. Pardo-Diaz C, Toro AL, Tovar SAP, Sarmiento-Garcés R, Herrera MS, Salazar C. Taxonomic reassessment of the genus Dichotomius (Coleoptera: Scarabaeinae) through integrative taxonomy. PeerJ. 2019 Aug 5;7:e7332.

74. Hudson RR, Boos DD, Kaplan NL. A statistical test for detecting geographic subdivision. Mol Biol Evol. 1992 Jan 1;9(1):138–51.

75. Leigh JW, Bryant D. popart: full-feature software for haplotype network construction. Methods Ecol Evol [Internet]. 2015 Sep 1 [cited 2023 Jun 14]; Available from: https://www.scinapse.io/papers/1946252112

76. Pritchard JK, Stephens M, Donnelly P. Inference of Population Structure Using Multilocus Genotype Data. Genetics. 2000 Jun 1;155(2):945–59.

77. Janes JK, Miller JM, Dupuis JR, Malenfant RM, Gorrell JC, Cullingham CI, et al. The K = 2 conundrum. Mol Ecol. 2017;26(14):3594–602.

78. Evanno G, Regnaut S, Goudet J. Detecting the number of clusters of individuals using the software structure: a simulation study. Mol Ecol. 2005;14(8):2611–20.

79. Earl DA, vonHoldt BM. STRUCTURE HARVESTER: a website and program for visualizing STRUCTURE output and implementing the Evanno method. Conserv Genet Resour. 2012 Jun 1;4(2):359–61.

80. Francis RM. pophelper: an R package and web app to analyse and visualize population structure. Mol Ecol Resour. 2017;17(1):27–32.

81. Oksanen J, Blanchet FG, Kindt R, Legendre P, Minchin P, O'Hara B, et al. Vegan: Community Ecology Package. R Package Version 22-1. 2015 Jan 1;2:1–2.

82. Hijmans RJ, Karney (GeographicLib) C, Williams E, Vennes C. geosphere: Spherical Trigonometry [Internet]. 2022 [cited 2024 Mar 4]. Available from: https://cran.r-project.org/web/packages/geosphere/index.html

83. Petkova D, Novembre J, Stephens M. Visualizing spatial population structure with estimated effective migration surfaces. Nat Genet. 2016 Jan;48(1):94–100.

84. Manni F, Guérard E, Heyer E. Geographic patterns of (genetic, morphologic, linguistic) variation: how barriers can be detected by using Monmonier's algorithm. Hum Biol. 2004 Apr;76(2):173–90.

85. Jombart T. adegenet: a R package for the multivariate analysis of genetic markers. Bioinformatics. 2008 Jun 1;24(11):1403–5.

86. Jackson ND, Morales AE, Carstens BC, O'Meara BC. PHRAPL: Phylogeographic Inference Using Approximate Likelihoods. Syst Biol. 2017 Nov 1;66(6):1045–53.

87. Rohlf FJ. The tps series of software. Hystrix Ital J Mammal. 2015 Jun 12;26(1):9–12.

88. Wilson JD, Zapata LV, Barone ML, Cotoras DD, Poy D, Ramírez MJ. Geometric morphometrics reveal sister species in sympatry and a cline in genital morphology in a ghost spider genus. Zool Scr. 2021;50(4):485–99.

89. Adams DC, Otárola-Castillo E. geomorph: an r package for the collection and analysis of geometric morphometric shape data. Methods Ecol Evol. 2013;4(4):393–9.

90. Scrucca L, Fop M, Murphy TB, Raftery AE. mclust 5: Clustering, Classification and Density Estimation Using Gaussian Finite Mixture Models. R J. 2016 Aug;8(1):289–317.

91. Goudey B, Geard N, Verspoor K, Zobel J. Propagation, detection and correction of errors using the sequence database network. Brief Bioinform. 2022 Nov 1;23(6):bbac416.

92. Viera C, Gonzaga MO, editors. Behaviour and Ecology of Spiders [Internet]. Cham: Springer International Publishing; 2017 [cited 2024 Jan 31]. Available from: http://link.springer.com/10.1007/978-3-319-65717-2

93. Kellogg J. Cenozoic tectonic history of the Sierra de Perijá, Venezuela-Colombia, and adjacent basins. Caribb-South Am Plate Bound Reg Tecton. 1984 Jan 1;162:239–61.

94. Warren DL, Cardillo M, Rosauer DF, Bolnick DI. Mistaking geography for biology: inferring processes from species distributions. Trends Ecol Evol. 2014 Oct 1;29(10):572–80.

95. García-Rodríguez A, Martínez PA, Oliveira BF, Velasco JA, Pyron RA, Costa GC. Amphibian Speciation Rates Support a General Role of Mountains as Biodiversity Pumps. Am Nat. 2021 Sep;198(3):E68–79.

96. Bartoleti LF de M, Peres EA, Fontes F von HM, da Silva MJ, Solferini VN. Phylogeography of the widespread spider Nephila clavipes (Araneae: Araneidae) in South America indicates geologically and climatically driven lineage diversification. J Biogeogr. 2018;45(6):1246–60.

97. Salgado-Roa FC, Gamez A, Sanchez-Herrera M, Pardo-Díaz C, Salazar C. Divergence promoted by the northern Andes in the giant fishing spider Ancylometes bogotensis (Araneae: Ctenidae). Biol J Linn Soc. 2021 Mar 1;132(3):495–508.

98. Boschman LM. Andean mountain building since the Late Cretaceous: A paleoelevation reconstruction. Earth-Sci Rev. 2021 Sep 1;220:103640.

99. Blandenier G. Ballooning of spiders (Araneae) in Switzerland: General Results from an Eleven-Year Survey. Arachnology. 2009 Mar;14(7):308–16.

100. Sobel JM, Chen GF, Watt LR, Schemske DW. THE BIOLOGY OF SPECIATION. Evolution. 2010 Feb 1;64(2):295–315.

101. Cong Q, Shen J, Borek D, Robbins RK, Opler PA, Otwinowski Z, et al. When COI barcodes deceive: complete genomes reveal introgression in hairstreaks. Proc R Soc B Biol Sci. 2017 Feb 8;284(1848):20161735.

102. Mallo D, Posada D. Multilocus inference of species trees and DNA barcoding. Philos Trans R Soc B Biol Sci. 2016 Sep 5;371(1702):20150335.

103. Corander J, Marttinen P. Bayesian identification of admixture events using multilocus molecular markers. Mol Ecol. 2006;15(10):2833–43.